PREPARATION, CHARACTERIZATION AND HYDRODESULFURIZATION (HDS) ACTIVITY OF MOLYBDENUM/SBA-15 CATALYSTS WITH INCREASED AND WELL DISPERSED MOLYBDENUM SPECIES

BY

ZAKARIYAH ABDULKAREEM JAMIU

A Thesis Presented to the

DEANSHIP OF GRADUATE STUDIES

KING FAHD UNIVERSITY OF PETROLEUM & MINERALS

DHAHRAN, SAUDI ARABIA

In Partial Fulfillment of the
Requirements for the Degree of

MASTER OF SCIENCE

In

CHEMISTRY

JULY, 2012

KING FAHD UNIVERSITY OF PETROLEUM & MINERALS

DHAHRAN 31261, SAUDI ARABIA

DEANSHIP OF GRADUATE STUDIES

This thesis, written by Mr. Zakariyah Abdulkareem Jamiu under the direction of his thesis advisor and approved by his thesis committee, has been presented to and accepted by the Dean of Graduate Studies, in partial fulfillment of the requirements for the degree of **MASTER OF SCIENCE IN CHEMISTRY**

Thesis Committee

Dr. Mohammed A. Al-Daous

(Advisor)

Dr. Mohammed Ali Morsy

(Member)

Dr. Nabil Othman Al-Yassir

(Member)

Dr. Abdullah J. Al-Hamdan
Department Chairman

Dr. Salam A. Zummo
Dean of Graduate Studies

30/7/12

Date

DEDICATION

To

My beloved parents for their care and prayers and to the memory of my late brother

ACKNOWLEDGMENT

First of all, I give thanks to Allah, the generally merciful and the especially merciful, for His favors in creating knowledge and then giving me the opportunity to seek knowledge.

My heartfelt acknowledgement goes to the chairman of my thesis committee Dr. Mohammed Abdulmajeed Al-daous for the origination of the work and his tremendous supports in carrying out the work. He shall be long remembered. Great thank to Dr. Mohammed Ali Morsy for his astuteness in pointing out the mistakes of the work and making the work more presentable. Further thanks to Dr. Nabil Othman Al-Yassir for his erudite contribution in suggesting ways of improvements.

I would like to appreciate some centers of excellences for allowing me access to use of their facilities in the course of the work. Centers for nanotechnology (CENT), water analysis (CEW) and petroleum refining (CPR) have been very supportive.

Furthermore, this acknowledgement is not complete without recognizing the Nigerian community in King Fahd University of Petroleum and Minerals. They have provided such halo of friendship that did not make me too homesick.

Finally and most importantly, I would like to appreciate King Fahd University of Petroleum and Minerals and her chemistry Department for providing the initial opportunity for me to study in her facilities and the subsequent award of Master degree of science in Chemistry. The amiable nature of the Chairman of Chemistry Department, Dr. Abdullah J. Al-Hamdan has been very helpful.

TABLE OF CONTENTS

LIST OF FIGURES

TITLE PAGE

LIST OF TABLES

TITLE PAGE

LIST OF SCHEMES

TITLE PAGE

ABSTRACT (ENGLISH)

NAME: **ZAKARIYAH ABDULKAREEM JAMIU**

TITLE OF STUDY: **PREPARATION, CHARACTERIZATION AND HYDRODESULFURIZATION (HDS) ACTIVITY OF MOLYBDENUM/SBA-15 CATALYSTS WITH INCREASED AND WELL DISPERSED MOLYBDENUM SPECIES.**

MAJOR FIELD: **CHEMISTRY**

DATE OF DEGREE: **MAY, 2012**

Mesoporous silica, SBA-15, materials containing varying amount of molybdenum loading up to 17% wt have been synthesized via co-condensation from acidic solution with non-ionic surfactant. Low angle XRD reveals that the structural integrity of the ordered mesoporous materials is still highly preserved after increased loading. As suggested by our various characterization techniques, the catalyst with 10% Mo loading shows the best dispersion of Mo active phase. All the catalysts show superior activity in the overall hydrodesulfurization (HDS) reactions of dibenzothiophene (DBT) in comparison with the impregnated catalyst used as a reference. Catalyst with 10% Mo shows the least activation energy (Ea) of 109kJ/mole which is about two-fold less than that of the reference catalyst. Kinetic analyses of the reaction data showed that the contribution of hydrogenation (HYD) route predominates over direct desulfurization (DDS) route in the HDS of DBT for all the catalysts.

MASTER OF SCIENCE
KING FAHD UNIVERSITY OF PETROLEUM & MINERALS
DHAHRAN, SAUDI ARABIA

ABSTRACT (ARABIC)

ملخص الرسالة

الاســــــــم: زكريا عبد الكريم

عنوان الدراسة: تحضير وتوصيف ودراسة الفعالية تجاه الازالة الهيدروجينية للكبريت للحفازات Mo-SBA-15 مع زيادة ونمطية توزيع الموليبدينوم

التخصـــــص: الكيمياء

تاريخ التخـرج: مايو- 2012

تم في هذه الرساله تحضير مركبات السيليكا (SBA-15) متناهية الصغر بحجم النانو والتي تحتوي على كميات مختلفة من الموليبدينوم بنسب وزنية تصل الى 17% . وتم التحضير باستخدام طريقة التكثيف المشترك من المحاليل الحمضية مع المنظمات غير أيونية السطح. قياسات التوصيف باستخدام حيود اشعة اكس اثبتت ان التركيب المسامي للمركبات المتناهية الصغر لم يتغير حتى بعد عملية التنقيح. كما ان التوصيف باستخدام طرق اخرى اثبت ان التنقيح بنسبة 10% أظهر أفضل توزيع للموليبدينوم النشط. جميع المواد الحفازة إظهرت نشاط عالي في الازالة الهيدروجينية للكبريت عند استخدام نموذج من مركب ثنائي بنزين الكبريت وذلك بالمقارنة بالحفاز المستخدم كمرجع. الحفاز المتضمن 10% من الموليبدينوم أظهر اقل طاقة تنشيط 109 كيلو جول لكل مول والتي تعتبر اقل مرتين مقارنة بالحفاز المستخدم كمرجع . التحليل الكيناتيكي لنتائج التفاعلات أظهر ان ميكانيزم التفاعل يغلب علية الهدرجة على ازالة الكبريت المباشرة في الازالة الهيدروجينية للكبريت في كل الحفازات المستخدمة في هذه الدراسة.

ماجستير العلوم

جامعة الملك فهد للبترول والمعادن

الظهران - المملكة العربية السعودية

Nomenclature

BCH	-Bicyclohexyl
BET	-BET theory aims to explain the physical adsorption of gas molecules on a solid surface
C_{DBT}	-Concentration of DBT at a given reaction time.
CHB	-Cyclohexylbenzene
CTAB	- Cetyltrimethylammonium bromide
CVD	- Chemical Vapor Deposition
DBT	-Dibenzothiophene
DDS	-Direct Desulfurization
DMDBT	- Dimethyl Dibenzothiophene
DMDS	-Dimethyl Disulfide
Ea	- Activation Energy
GC-MS	-Gas Chromatography Mass Spectrometer
HDS	-Hydrodesulfurization A process for lowering the sulfur content of petroleum and similar products by catalytic hydrogenation.

HPA	-Heteropolyanions
HYD	-Hydrogenation
k	-Reaction rate constants
K	-Equilibrium adsorption constants of DBT over the catalytic active sites
MCM-41	-Mobil Crystalline Materials
MoS_2	-Molybdenum disulfide
MPa	-megapascals is a unit of pressure
ppm	-part per million
R_{DDS}	-rate of direct desulfurization
R_{HYD}	-rate of hydrodenation
SBA-15	-Santa Barbara Amorphous type material
TEM	-Transmission Electron Microscope
THDBT	-Tetrahydrodibenzothiophene
ULSD	-Ultra Low Sulfur Diesel
XRD	-X-ray Diffraction

CHAPTER 1

1.1 INTRODUCTION

As the drive for clean burning fuel is intensified with strict regulations in many countries of the world, researches into the production of ultra low sulfur diesel (ULSD) have attracted considerable attention. Although meeting these fuel standards is of immense benefit for our health and environment, the petroleum refiners are facing uphill task in order to overcome the economic and operational challenges that accompanied the regulations [1-3]. One of the greatest concerns is the declining quality of the crude oil available to the refiners as feedstock vis-a-vis the increasing demand for the ultra low sulfur fuels. This presents a great dilemma. Refiners are, therefore, constrained to deliver high quality diesel products from low quality feedstock. To this end, a lot of efforts have been geared.

Among several approaches that have been made, the development and application of more active and stable hydrotreating catalyst is favored [4]. Though the classic transition metal sulfide-based formulation usually supported on alumina has remained a household name in the hands of refiners as a response to the challenges of hydrodesulfurization (HDS), conventional catalysts still encounter difficulty in the HDS of least reactive alkyl

dibenzothiophene to ultra low level. It is estimated that in order to bring the sulfur level to <1ppm as may be demanded for fuel cell application, about seven times more active catalysts are required [3].

A large number of research studies in recent past have focused on finding more effective catalysts for the desulfurization of least reactive sterically hindered alkyl dibenzothiophenes, DBTs. Despite some interesting results concerning the catalytic activity of new phases such as carbides [5], phosphides [6], or nitrides [23], the classic sulfide-based formulations, comprising of molybdenum sulfide (or tungsten sulfide) phase promoted by cobalt or nickel and usually supported on alumina [7], appear to be the most promising in responding to the challenges. Major catalyst companies have developed highly active molybdnenum-based HDS catalysts in the market. Detail of this has been reviewed [8]. In particular, the emergence of much more active Mo-based catalysts, such as NEBuLA (considered as a breakthrough in hydrotreatment) [9], SMART [10], BRIM [11, 12], to mention a few, illustrates the fact that MoS_2-based materials, although, having been around for several decades, still have a great potential.

In recent time, a number of research studies have explored ways of enhancing the performance of supported catalysts by increasing the active phase loading. Nevertheless, the need to ensure high dispersion of active phase species that can afford complete sulfidation demands good understanding and control of preparation variables. In particular, improvements in catalyst impregnation and preparation techniques [13] and use of modified supports [14] are among numerous methods that have been used to increase the concentration of more active type II sites on the surface of the support. Moreover, clear understanding of the nature and structure of the active sites on the

support, textural characteristics of the support and their effects are keys to the development of highly active hydrodesulfurization catalysts [15-17]. When the interaction between the support and active metal is strong, the reducibility and sulfidability of active phase become difficult. This often leads to formation of less active type I sites on alumina supports.

Silica which is the support for the proposed work is known for its higher surface area and weak interaction with Mo active species in comparism with alumina. This low support-active phase interactions in SiO_2 can stimulate the formation of more active Co-Mo-S II/Ni-Mo-S-II phase [18] with improved synthesis approach. In recent time, nano-porous silica based material such as MCM-41, Al-MCM-41, and SBA-15 have attracted some attention as supports for Co and Ni promoted MoS_2 catalyst [19-22]. The high surface area of these nano-pore materials accommodates high CoMo or NiMo loading without the restricted access of the zeolite structure to bulky molecules. Their well defined textural properties are good factors for dispersion of MoS_2 particles.

1.2 RESEARCH OBJECTIVES

The following are the objectives of the thesis:

a.) To synthesize supported high loading and highly dispersed MoS_2 catalyst on ordered mesoporous silica-SBA-15

b.) To characterize the catalyst in order to ascertain the chemical form, the amount and the dispersion of the active ingredient in the active phase.

c.) To evaluate the activity of the catalyst on hydrodesulfurization (HDS) of dibenzothiophene (DBT).

CHAPTER 2

LITERATURE REVIEW

2.1 REVIEW OF DESULFURIZATION CATALYST TECHNOLOGIES

In an attempt to meet the growing demand for ultra low sulfur fuel and satisfying the stricter regulation of sulfur standards around the world, a number of new concepts and technologies have been developed in the last 20 years in addition to the choice of revamping the conventional hydrotreaters. It has been reported that most of the hydrotreaters that were installed to meet the 1993 low sulfur requirement (500ppm) can be revamped for ultra low sulfur diesel (10ppm) production with reasonable increase in operational and capital costs [24]. Though several options such as increasing the severity of operating conditions, increase catalyst volume, removal of H_2S from recycle gas, improve feed distribution in the reactor by using high efficiency vapor/liquid distribution trays, and use of easier feeds have been explored [8], the use of highly active catalysts has been given a lot of importance. The use of improved hydrotreating catalysts with high activity can improve considerably the desulfurization performance of existing hydrotreating units.

New improved catalysts have been developed by major catalyst companies and introduced into the market. Using co-impregnation in aqueous solution containing Co, Mo, orthosphosphoric acid and carboxylic acid and HY–Al_2O_3, Cosmo Oil Co. Ltd. developed C-606A with 3 times higher HDS activity compared to the conventional CoMoP/Al_2O_3 [25]. Akzo Nobel came up with the STARS catalyst series [8], which almost doubled the HDS activity. In recent time, the company introduced to the market a new catalyst, the NEBuLA, which is considered a breakthrough in hydrotreating catalysts [9]. The new catalyst which is made of unsupported bulk sulfides of group VIII and group VI metals is almost 4 times as active as conventional gas oil hydrotreating catalysts. ART has introduced the sulfur minimization by ART (SMART) catalyst system, with a remarkably high activity than predecessor hydrotreating catalysts [10].

A number of catalysts such as TK-573, TK-574, TK-911 and TK-915, which not only significantly improved desulfurization activity, but also tackled density and aromatics reduction, have been developed by Topsøe. Recently, Topsøe has developed a new catalyst preparation technology, giving highly active hydroprocessing catalysts. This new proprietary BRIM technology not only optimizes the brim site hydrogenation functionally, but also increases the type II activity sites for direct desulfurization [11]. The first two commercial catalysts based on the brim technology were Topsøe's TK-558 BRIM (CoMo) and TK-559 BRIM (NiMo) for FCC pretreatment service. This was followed by a new series of high performance TK-576 BRIM (CoMo), TK-575 BRIM (NiMo) and TK-605 BRIM catalysts for ultra low sulfur diesel production and for hydrocracker feed pretreatment [8]. Research on developing improved catalyst for

desulfurization is an active research area and is expected to continue to play a key role in achieving the clean fuel program

2.2 DISTRIBUTION OF SULFUR COMPOUNDS IN THE DIESEL FEEDS

Analyses of petroleum feeds conducted with the aid of high resolution gas chromatography equipped with sulfur selective detectors have shown that liquid fuels contain a large number of sulfur compounds of varying reactivities. The common types of sulfur compounds in liquid fuels are outlined in the table 2.1.

Table 2.1: Typical Sulfur Compounds and Corresponding Refinery Streams for Fuels [3].

Sulfur compounds	Refinery streams	Corresponding fuels
Mercaptanes, RSH; sulfides, R2S; disulfides, RSSR; thiophene (T) and its alkylated derivatives, benzothiophene	SR-naphtha; FCC naphtha; coker naphtha	Gasoline (BP range: 25–225 °C)
Mercaptanes, RSH; benzothiophene (BT), alkylated benzothiophenes	Kerosene; heavy naphtha; middle distillate	Jet fuel (BP range: 130–300 °C)
Alkylated benzothiophenes; dibenzothiophene (DBT); alkylated dibenzothiophenes	Middle distillate; FCC LCO; coker gas oil	Diesel fuel (BP range: 160–380 °C)
Greater than or equal to three-ring polycyclic sulfur compounds, including DBT, benzonaphthothiophene (BNT), phenanthro[4,5-b,c,d]thiophene (PT) and their alkylated derivatives and naphthothiophenes (NT)	Heavy gas oils; vacuum gas oil; distillation resides	Fuel oils (non-road fuel and heavy oils)

In comparism with the commercial transportation fuel in US, Ma et al in 2002 have established that the following sulfur compounds as depicted in Figure 2.1 are prevalent in the finished products of gasoline, jet fuels and diesel fuels [26, 27]. It is obvious from figure 2.1 that in each of the fuels, what is left of sulfur compounds in the finished products are those that have lower reactivities among all the sulfur compounds in the corresponding feed e.g., naphtha range for gasoline, kerosene range for jet fuel, and gas oil range for diesel fuel [3].

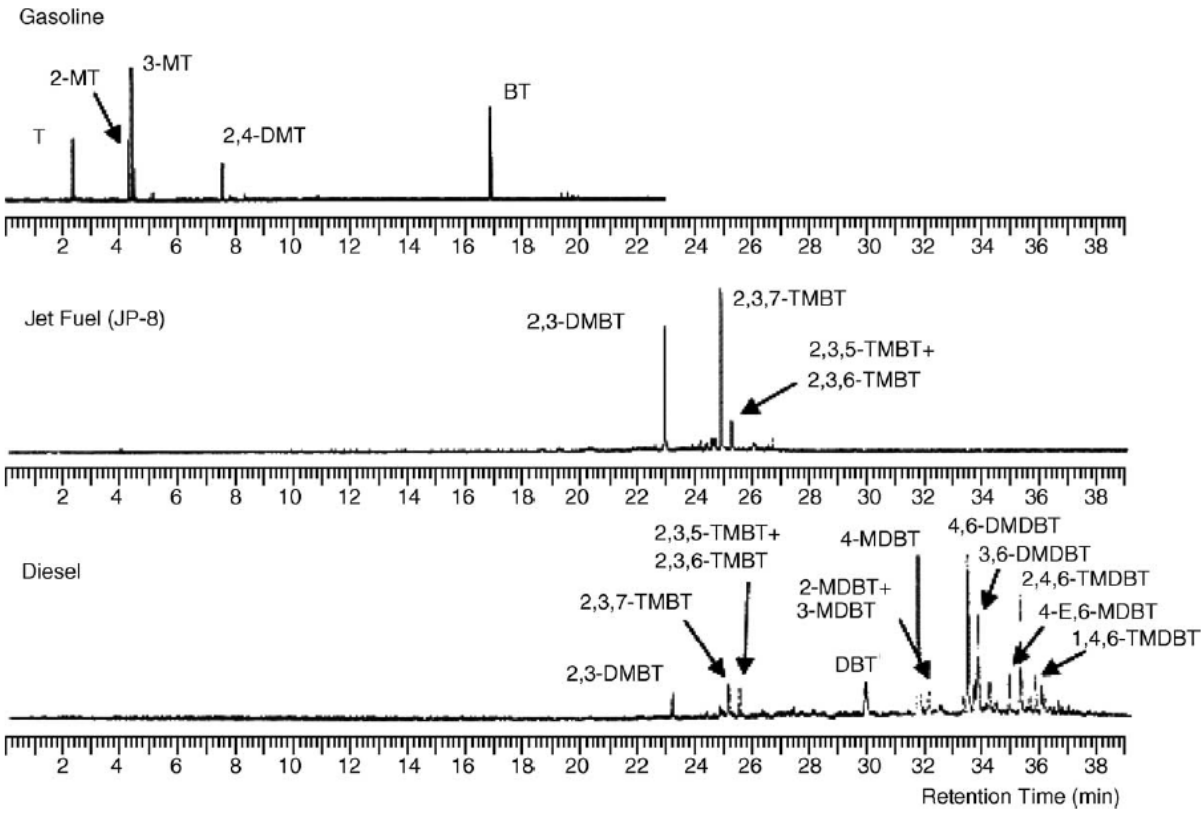

Figure 2.1: Sulfur Compounds in Commercial Gasoline, Jet Fuel and Diesel Fuel identified by GC-FPD Analysis coupled with GC-MS and Reaction Kinetic Analysis [27].

Among the thiophenic group, two subdivisions can be identified: the benzothiophenes (BTs) and the dibenzothiophenes (DBTs). These and their derivatives are among the least reactive sulfur compounds in the liquid fuels. So the target of deep desulfurization and ultra-deep desulfurization is to remove these refractory sulfur compounds that exist in the current gasoline and diesel fuels to ultra low level or zero.

2.3 HDS REACTIVITY OF SULFUR COMPOUNDS

It has been established by several research studies that the relative reactivities of thiophenic sulfur compounds are significantly different [28-30]. This could be attributed to the conjugative interaction between lone pair of electrons on sulfur atoms and the π–system of the aromatic ring. Benzothiophenes (BTs) and its alkyl derivatives are generally faster to disulfurize than the corresponding dibenzothiophene and its alkyl derivatives. Among the isomers of DBTs, the β-isomers (e.g. 4, 6-DMDBT) are less reactive and more difficult to disulfurize [31, 32]. In fact, there is a good agreement from experimental data that over typical CoMo/alumina and NiMo/alumina hydrotreating catalysts, 4, 6-DMDBT is of an order of magnitude less reactive than dibenzothiophene (DBT) [30, 33-35]. It has also been established that the size of alkyl substituents at β-position to sulfur atom in the DBTs has a large effect on reactivity of alkyl DBTs and its desulfurization [36]. This trend has been attributed to the steric hindrance of the substituent alkyl group which prevents interaction between sulfur atom and the catalytic active sites [30], and the electronic inductive effects between the alkyl groups on the ring and the sulfur atom thereby enriching electron density on the sulfur.

2.4 MECHANISM OF HDS REACTIONS

In order to design an effective catalyst for the production of ultra low sulfur diesel (ULSD) fuel, the various kinetic pathways of hydrodesulfurization (HDS) reactions must be understood. For a typical dibenzothiophene (DBT) molecule, it has been established that the HDS reaction proceeds through two parallel and consecutive routes (**scheme 2.1**): (i) direct desulfurization (DDS) which yields biphenyl-type compounds (BP), and (ii) desulfurization through hydrogenation (HYD) which gives tetrahydrodibenzothiophene (THDBT). Depending on the reaction condition, THDBT or both THDBT and may be further hydrogenated to yield cyclohexylbenzene-type compounds (CHB) [29, 37, 38]. Subsequent hydrogenation of CHB may yield bicyclohexyl (BCH). However, depending on the reactant (DBT or 4, 6-DMDBT), the contribution of the two pathways to the overall HDS may be very different. Under conventional HDS conditions [39], the DDS pathway contributed 80% to the overall HDS of DBT, while only 20% to the HDS of 4, 6-DMDBT. It was also found that the presence of methyl groups in the 4 and 6 positions in 4, 6-DMDBT inhibited the DDS pathway, whereas the HYD pathway was hardly affected [30, 34, 39].

The HYD pathway predominates with the introduction of alkyl substituents in the in the 4 and , or 6-positions of the DBT molecules [61,62]. Meille V. et al reported that the partial saturation changes the spatial configuration of the molecule making previously sterically hindered sulfur atom more accessible for effective adsorption on the active site and subsequent reaction [63].

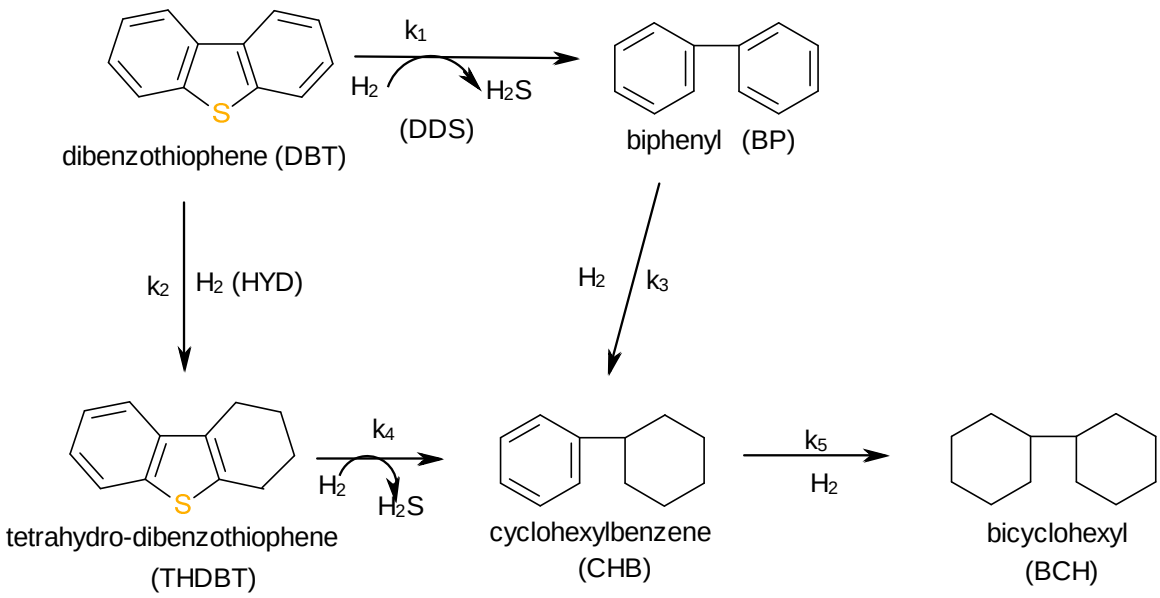

Scheme 2.1: Typical Hydrodesulfurization of Dibenzothiophene.

From the theoretical stand point, hydrogenation of biphenyl and its derivatives to cyclohehexyl benzene may take place especially at high conversion. However, at moderate conversion, the chances of BP hydrogenation are significantly low in the presence of DBT, because DBT successfully competes with BP for the hydrogenation sites of the catalysts [64, 65]. More so on Ni promoted catalyst.

2.5 KINETICS OF HYDRODESULFURIZATION (HDS)

The kinetics of HDS reactions has been the focus of many researchers. Langmuir-Hinshelwood (L-H) type kinetic equations which assume competitive adsorption have been developed for HDS of pure sulfur compounds [66, 67]. **Table 2.2** displays some important kinetic equations that have been reported for the HDS of DBT in the literature [8]. Here, the contribution from both hydrogenolysis and hydrogenation are summed together. On the other hand, researchers have also proposed a separate L-H equation for both hydrogenolysis and hydrogenation for the HDS of DBT [66, 68]. For instance, Farag H. proposed the following separate L-H equations for direct desulfurization (DDS) and hydrogenation (HYD) for the HDS of DBT with two kinds of catalytic active sites [68]:

$$R_{DDS} = \frac{k_1 K_1 C_{DBT}}{1 + K_1 C_{DBT} + \cdots} \quad \text{and} \quad R_{HYD} = \frac{k_2 K_2 C_{DBT}}{1 + K_1 C_{DBT} + \cdots}$$

Here, R_{DDS} and R_{HYD} are the rate of direct desulfurization (DDS) and the rate of hydrogenation (HYD) of DBT, respectively. K_1, k_1 and K_2, k_2 are the equilibrium adsorption constants of DBT over the catalytic active sites and the reaction rate constants for DDS and HYD, respectively. C_{DBT} is the concentration of DBT at a given reaction time.

Summation of the two rate equations gives the kinetic expression for the apparent overall HDS conversion. The two-route kinetic model has been found to describe satisfactorily the HDS of alkyl DBTs present in LCO [69].

Table 2.2: Kinetic Expression for Middle Distillate Range of Sulfur Compounds [8].

Catalysts	Conditions	Rate Expression
CoMo/alumina	200-240°C	$r_{HDS} = k\frac{k_{DBT}P_{DBT}}{(1+k_{DBT}P_{DBT}+k_{H2S}P_{H2S})2} \cdot \frac{k_{H2}P_{H2}}{(1+k_{H2}P_{H2})}$
NiMo type II	350°C, 50 bar	$r_{HDS} = \frac{k'_{DDS}C_{DBT}}{(1+k'_{DDS,N}C_{CZ}+K'_{DDS,N}C_{TC})} + \frac{k'_{HG}C_{DBT}}{(1+k'_{HG,N}C_{CZ}+k'_{HG,N}C_{TC})}$
CoMo/alumina (monolith)	270-300°C, 60-80 bar	$-r_{DBT} = \frac{kK_{DBT}k_{H2}C_{DBT}C_{H2}}{(1+K_{DBT}C_{DBT}+K_{H2}C_{H2}+K_{H2S}C_{H2S})^2}$

2.6 SUPPORTED CATALYST

The active phase in a HDS catalyst sample is usually deposited on the surface of another material called support. The support material usually provides high surface area to maximize the active phase dispersion and to provide mechanical strength to the catalyst. They are usually sourced from various oxides such as Al_2O_3, TiO_2, ZrO_2, MgO, SiO_2, zeolites and compounds such as carbon. Alumina the most widely used of this support materials still remains the industry's favorite because of its favorable chemical, physical, and mechanical properties on one hand, and its activity response, availability and cost on the other hand [18].

For several decades, CoMo and NiMo/alumina have been used in industrial refining plants as HDS catalysts. Since the proposal of Topsøe and co-workers [40], there has been a growing interest in the so-called CoMoS or NiMoS phases, in which Co(Ni) decorates the edge sites of highly dispersed MoS_2 particles. These phases may be catalytically active sites in Co(Ni)–Mo sulfide catalysts and many catalytic and spectroscopic aspects of Co(Ni)–Mo sulfide catalysts have been interpreted in terms of these phases. Candia et al [41] differentiated between two CoMoS phases, Type I and Type II, depending on their intrinsic HDS activity. CoMoS Type II, which was formed by high-temperature sulfidation at ~600-1000 C°, was about twice as active as Type I formed by sulfidation at ~400 °C. More recently Okamoto et al. [42, 43] reported the formation of a third type of Co–Mo–S phase (Co–Mo–S Type III) with high intrinsic HDS activity when SiO_2-supported CoMo catalyst was sulfided with 10% H_2/He. The structure of this phase (Co–Mo–S type III) was suggested to consist of dinuclear Co

sulfide cluster with S-dimer between two Co atoms and situated on the Mo-edge of MoS_2 particles [8].

It has also been reported by several authors that variation of the support influences the electronic and catalytic properties of supported NiMo and CoMo sulfide catalysts [40]. This is because changes in supports usually lead to variations in active phase-support interaction which in turns influence the dispersion and morphology of active components. When the interaction between the support and the active metal is strong, the reducibility and sulfidability of the active phase will be retarded. For conventional CoMo-S and NiMo-S, studies have shown that the strong interactions between the molybdate and the support lead to formation of low active type I structure having some remaining Mo-O-Al linkages after sulfidation [44-47]. This may mean that a further increase in the HDS activity of supported sulfide catalysts can be achieved by changing the support.

The development of new supports has received great attention because of the need to develop better HDS catalysts [48]. TiO_2, ZrO_2, MgO, SiO_2, zeolites, carbon and other materials of high surface areas and good properties have been developed and tested [49, 50]. TiO_2 and ZrO_2 supported MoS_2 catalysts present, respectively, three to five times higher hydrodesulfurization and hydrogenation activities than alumina supported ones with an equivalent Mo loading per nm^2 [51]. However, for a considerable period of time, the specific surface area of such oxides remained below 100 m^2/g (after calcination at 500 °C) restricting the interest on such supports. Within the last decade, many improvements in the preparation of these oxides were achieved and supports with higher specific surface area and larger pore diameters were obtained.

Silica, another common support often used, is known for its higher surface area in comparison with alumina. However, its weak interaction with Mo active species usually leads to poor dispersion of the active phase. Modification of silica by mixing with other supports having favorable properties have shown significant increase in activity and it has attracted some considerable attention [8]. Amorphous materials SiO_2-Al_2O_3 have shown some considerable HDS activity over zeolites in the HDS of 4, 6-DMDBT when mixed with NiMo/alumina catalyst [52]. The addition of SiO_2 increases the surface area of alumina support and introduces acid sites required for some hydrotreating reactions. In addition, SiO_2 reduces support-active phase interactions which stimulate the formation of more active Co-Mo-S II/Ni-Mo-S-II phase [18]. Impregnation of the metals and thermal treatments may, however, be more critical [18].

Of recent, researchers have turned their attention towards ordered mesoporous materials. This new class of porous solids posses uniform pore sizes (1.5-40nm), large surface areas (up to 2500m^2/g) and tunable structures [53, 54]. They are among the most promising candidates as nano-reactors of large molecules [55]. Nano-porous silica based material such as MCM-41, Al-MCM-41, and SBA-15 have attracted some attention as supports for Co and Ni promoted MoS_2 catalyst [19-22]. The high surface area of these nano-pore materials accommodates high CoMo or NiMo loading without the restricted access of the zeolite structure to bulky molecules. Their well defined textural properties are a good factor for dispersion of MoS_2 particles [8]

2.7 PREPARATION METHODS

The performance of a catalyst is strongly influenced by preparation procedures [56]. Typical HDS catalyst preparation involves the use of incipient-wetness or pore-volume impregnation of an aqueous Mo-solution. Promoter ions are either co-impregnated or impregnated after initially sulfidizing the supported Mo species [7]. Meanwhile, to reduce the interaction of the promoting ions with the support and to delay the sulfidation of the promoter ions in order not to produce sulfide species independent of the MoS_2, chelating agents such as nitrilotriacetic acid are used [57]. However, high Mo loading and dispersion cannot be obtained by such a procedure because the formation of large particles occurs readily under the activation conditions [7].

Conventional methods of preparation of industrial catalysts usually use oxide precursors which are sulfided into their active form. In this case, the nature of these oxides species and their distribution on the surface of supports are key factors for their activation and performance during application. For Mo based catalysts, the presence of bulk MoO_3 or MoO_4 particles is counterproductive when high metal active phase are deposited on the support. The active species are best deposited as isolated oxoanions. Unfortunately, the support materials are not inert towards the precursors of the active phase, they can interact to produce heteropolyanions (HPA) which may crystallize at increased loading leading to poor dispersion of active phase [15].

One method of overcoming this challenge is the use of aqueous solution reaction for the synthesis of highly loaded supported and unsupported hydrotreating catalysts. Bezverkhy I. et al used thiomolybdate precursor $(NH_4)_2MoS_4$) and hydrazine as a reductant in aqueous medium to prepare MoS_2 with very high HDS activity [58, 58]. The

key to this synthesis is the control of pH of the solution and temperature of the reaction. This preparation method can be conducted in the presence of support slurry or promoter ion to produce highly active promoted hydrotreating catalysts [58].

Highly active HDS catalysts were also prepared by use of surfactant-assisted synthesis method. For instance, in the reduction of the thiomolybdate by hydrazine, cetyltrimethylammonium bromide (CTAB) was added to the reaction mixture. This resulted in MoS_2 nanoparticles with low stacking and high specific surface area of up to $210 m^2 g^{-1}$. Further promotion with Ni or Co results in catalyst with HDS activity of about five times higher than that of a commercial reference catalyst in the HDS of 4, 6-DMDBT [70].

Another method for preparing an active HDS catalyst is a sonochemical synthesis, which was demonstrated to yield substantially high loading and dispersion of MoS_2 [59]. Moon et al. reported that sonochemically prepared MoS_2/Al_2O_3, at a Mo loading of 25 wt%, showed a five-fold higher activity than that of a corresponding catalyst prepared by a conventional impregnation method in the HDS of model DBT compounds [59]. Also another method for improving catalyst activity is to introduce a promoter, e.g., Co, to MoS_2 catalysts by chemical vapor deposition (CVD) such that the promoter interacts intimately with the MoS_2 surface. For example, a catalyst prepared by thermo decomposition of $Co(CO)_3(NO)$ on MoS_2/Al_2O_3 showed twice as high an activity as the catalyst promoted by impregnation in the HDS of thiophene [60]. The enhanced activity can be attributed to the exclusive decoration of Co on MoS_2 edge sites, which eventually leads to an increase in the amount of catalytically active CoMoS phase. Similar results were obtained by Okamoto et al. with model CoMoS catalysts supported on various

supports, which were prepared using the CVD method. More recently, Moon et al [61] combined sonochemical synthesis and CVD to prepare new highly dispersed and promoted catalysts.

2.8 CATALYST ACTIVATION

Hydrotreating catalysts usually go through activation stage for better performance in hydrotreating reaction. Conventional procedure uses dimethyl disulfide (DMDS) as a spike agent with straight run gas oil to convert the oxide catalyst to a more active sulfide form. The sulfidation protocol differs from large scale industrial settings to a laboratory scale. In the laboratory, a mixture of H_2/H_2S is usually employed for the sulfidation of oxide catalysts under a control temperature program. The process can be ex situ or in situ and kinetic studies are either performed under high atmospheric pressure or under high pressure of about 4MPa [71].

CHAPTER 3

EXPERIMENTAL

3.1 SYNTHESIS OF Mo-SBA-15 SUPPORTED CATALYST

Mo-SBA-15 materials containing molybdenum metal was synthesized via co-condensation from aqueous solution containing the metal and silica precursors. Pluronic-123 [$EO_{20}PO_{70}EO_{20}$, Aldrich] was used as structure directing agent while tetraethylorthosilicate [TEOS, Sigma-Aldrich] and ammonium molybdate tetrahydrate [$(NH_4)_6Mo_7O_{24}.4H_2O$, Fischer Scientific] were used as silicon and metal precursors respectively. In a typical synthesis, appropriate amount of Pluronic-123 was dispersed in hydrochloric acid (HCl) solution. The dispersion was stirred at room temperature for about one hour. This is designated as solution A. For the solution B, appropriate amount of heptamolybdate was dissolved in de-ionized water and stirred at room temperature for about two hours. Solutions A and B were then contacted while stirring at 35°C and appropriate amount of TEOS was added to the mixture and the mixture was allowed to ripe. Subsequently, it was aged at 90°C. The solid product was recovered by filtration and dried. It was subsequently calcined at 550°C for 4hours. The synthesis strategy is designated in **scheme 2.1**.

Mo-SBA-15 prepared by impregnation for comparison purpose was synthesized as follows: About 3g of calcined pure SBA-15 was impregnated with an aqueous solution of the molybdenum precursor, using the needed concentration to achieve the desired Mo content assuming total incorporation. The wet solid was then dried and calcined in air under static conditions at 550°C for 4 h using a ramp step of 2°C per min.

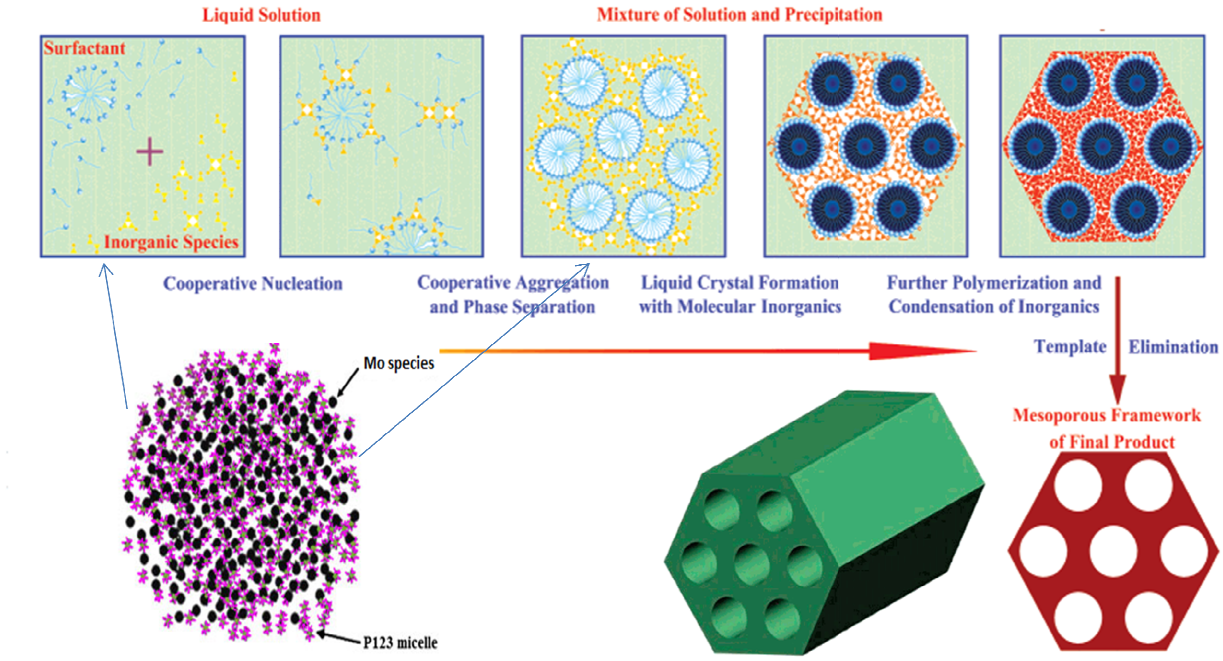

Scheme 3.1: Synthesis Strategy of Mesoporous Materials via Cooperative Self-assembly

3.2 SAMPLE CHARACTERIZATION

3.2.1 Elemental Composition: Bulk metal content was determined by atomic absorption spectroscopy. Typically, 50mg of the sample was digested using aqueous hydrofluoric acid and nitric acid mixture. The samples were diluted to the appropriate concentrations. Mo (1000mg/L in water) was used to calibrate the equipment.

3.2.2 N2 Adsorption/Desorption Isotherm: Nitrogen adsorption/desorption isotherms were acquired using porosimeter. Specific surface area was calculated using BET method and pore size distributions were calculated using BJH method assuming cylindrical pore geometry.

3.2.3 XRD: The x-ray powder diffraction patterns (XRD) were collected on a diffractometer using the Cu Kα line for both the low and wide angle in the 2θ range. The XRD data were recorded in the 2θ range from 0.85 with a step size of 0.0005 for low angle analysis and in the 2θ range from 10.00 using a step size of 0.01 for high angle analysis.

3.2.4 DR UV-vis Spectra: Diffuse reflectance UV–vis spectra (DR UV–vis) were recorded under ambient conditions in the wavelength range from 200 to 600 nm. DR UV–vis spectra were collected using Evolution 600 181001.

3.2.5 FT-IR Spectroscopy: infra red spectra of different samples were also scanned from 500 to 4000 cm^{-1}.

3.3 ACTIVATION OF THE CATALYSTS

Before the catalytic activity tests, the catalysts were sulfided ex situ in a tubular furnace at 400°C for 1.5 hours in a stream of 10% H_2S in a balanced H_2. The presulfiding step is necessary to convert the catalyst from oxide form to sulfide form which is more active under the conventional reaction system. The sulfided catalyst was transferred quickly into the batch reactor containing the feed.

3.4 ACTIVITY MEASUREMENT

Activity measurement was done by carrying out reactions in a 250ml autoclave stirred batch reactor at three different temperatures of 325, 350 and 375°C. In a typical reaction, 120ml of the feed (about 5000 ppm DBT in decane) was charged into the reactor with 0.5g of the sulfided catalyst. The system was purged with nitrogen in order to detect any leak and it was later purged three (3) times with hydrogen. Subsequently, the hydrogen pressure was adjusted to 4MPa and the stirring rate was 500rpm. The reaction system was heated to the desired temperature and allowed to proceed for 3hours. During the reaction, liquid samples of 3-5ml were withdrawn at 30 minutes intervals for 3hours. Liquid samples were analyzed with Agilent gas chromatograph fitted with appropriate column and detector. Mass spectrometer detector was used to identify the reaction products. These results were used in the kinetic study.

CHAPTER 4

RESULTS AND DISCUSSION

4.1 MOLYBDENUM CONTENT

Though a lot of syntheses were made in the course of this experiment, only the ones used in the reaction will be discussed. **Table 4.1** summarizes the synthesis conditions used for the preparation of different molybdenum-containing Mo-SBA-15 materials used in the reaction. In order to obtain different metal loadings on the mesostructured materials, the molybdenum content in the initial gel mixture has been varied from 15% to 25% weight of Mo/SiO_2 to determine the optimum limit of incorporation. From **Table 4.1**, it is obvious that there is a direct relationship between the initial metal loading in the synthesis gel and the metal incorporation into the final material. However, the incorporation efficiency peaked at 71% for all the syntheses which in our understanding is due to the strong acidic media that discourage the anchoring of the molybdenum metal to the silica matrix as previously reported [72-74].

Table 4.1: Synthesis Conditions and the Elemental Compositions of the Materials.

S/N	synthesis condition		Composition in the final material	
	% Mo[a]	HCl (N)[b]	% Mo[c]	η (%)[d]
S1	15	1.06	6	40.00
S2	15	0.88	8	55.67
S3	15	0.71	10	69.00
S4	20	1.24	7	37.20
S5	20	1.06	10	47.50
S6	20	0.88	12	59.30
S7	20	0.71	14	71.15
S8	25	1.24	13	53.16
S9	25	1.06	16	64.80
S10	25	0.88	17	68.08
S11	25	0.71	18	71.44

[a] % Mo in the initial synthesis gel mixture
[b] Normality of HCl in the synthesis mixture
[c] % Mo in the final material after calcination measured by AAS
[d] Mo incorporation efficiency

In order to gain more insight into the contribution of the synthesis parameters to the incorporation efficiency, further syntheses were done by varying the acidity of the synthesis gel. The strong effect of pH on the incorporation of the metal into the mesoporous silica matrix becomes most obvious. For instance, in the 20% loadings in the synthesis gel, samples S4-S7, the incorporation efficiency rose from 37% to 71% by simply lowering the acid concentration from 1.24N to 0.71N. The large effect of the small decrease of about 0.5N underscores the effect of pH. This trend has been represented in **Figure 4.1**. The influence of slight change in pH and varying amount of loading in the synthesis gel becomes more noticeable. Similar trends are observed for 15% and 25% loadings in the synthesis gel. This confirms the previous claims that lower pH opposes the incorporation of molybdenum metal into the SBA-15 matrix [72]. The effect of stirring rate and ripening time were also investigated and the results are consistent with the literature.

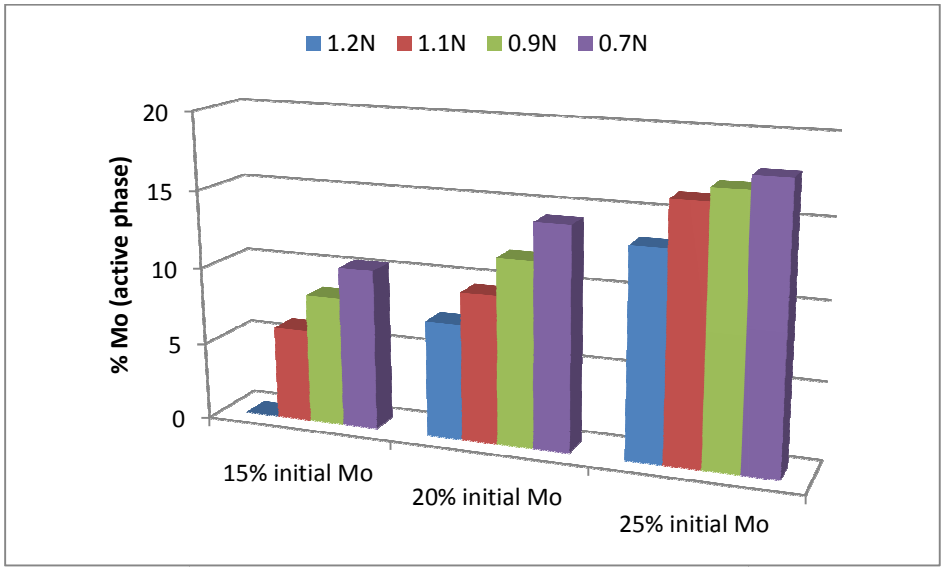

Figure 4.1: Percentage Mo active phase as a Function of Acidity and Amount of Mo in the initial Synthesis Medium.

4.2 X-RAY DIFFRACTOGRAMS

4.2.1 Oxide Catalysts

Figures 4.2 to 4.4 below depict the effect Mo loadings on the structure of SBA-15 materials by examining their diffraction patterns. For the 15% Mo loading in the initial synthesis gel, the low angle XRD peaks for the calcined samples give intense signals leading to a diffraction pattern characteristic of the p6mm symmetry of the hexagonal array of pores in the SBA-15 topology, Figure 4.2 (a). The presence of three clear reflections, corresponding to the 100, 110 and 200 planes, is indicative of the high ordering achieved in the mesoscopic range and that structural integrity of the ordered mesoporous material is still preserved as the amount of Mo loading increases from 6% in Figure 4.2a(I) to 10% in Figure 4.2a(III). The foregoing results demonstrate that the original pore structure and the long-range periodicity order of the pure SBA-15 are not affected despite 10% Mo loading.

In the wide angle region where Mo oxide peaks are expected, Figure 4.2b, there is a complete absence of any reflections corresponding to oxide of Mo except the background signals caused by amorphous silica. This trend is maintained as Mo loading is increased from 6% in Figure 4.2b (I) to 10% in Figure 4.2b (III). The occurrence of this trend suggests a complete absence of crystalline domains of molybdenum oxide or, if present, the crystal sizes are too small and uniformly dispersed to be detected by X-ray diffraction.

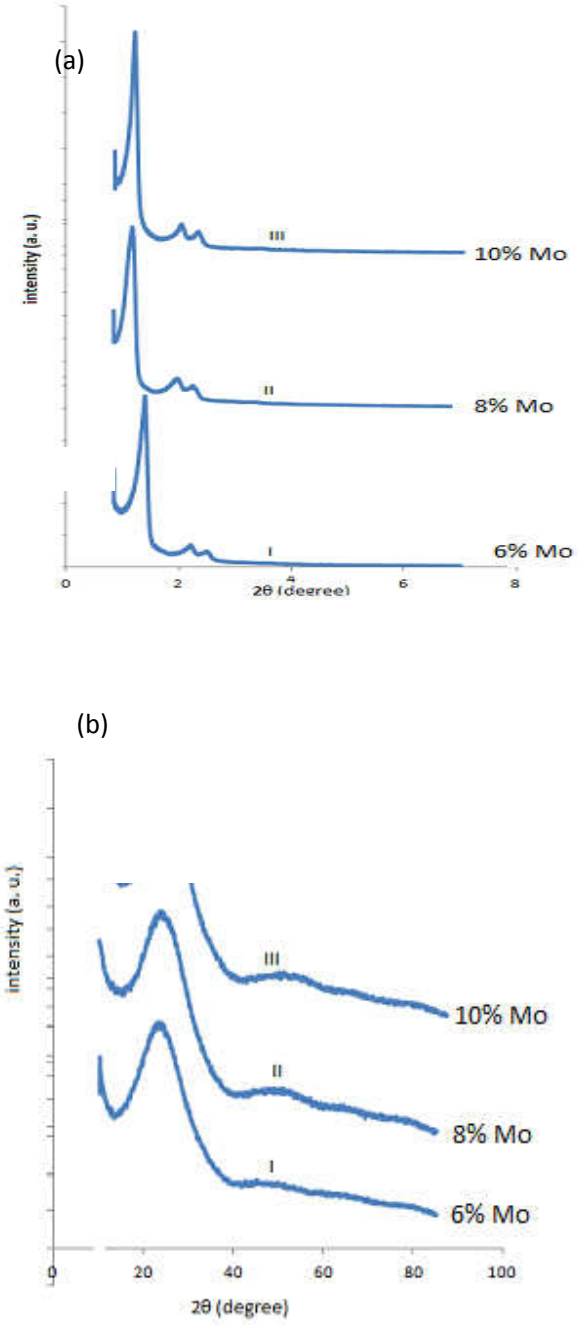

Figure 4.2: XRD Patterns of 15% Mo initial loading in the Synthesis Gel at various Acid Concentrations for (a) low Angle and (b) wide Angle Diffractograms.

In order to see the effect of higher loadings on structure of SBA-15, more synthesis were made with increased loading up to 17% Mo on SBA-15 support. The low angle diffractograms of these materials are compared in Figure 4.3. In all the samples, the structures of SBA-15 were largely preserved even up till the high loading of 17% Mo. In the wide angle diffraction, Figure 4.4, diffraction lines corresponding to reflections of MoO_3 phase are observed for all other samples except for (a) in Figure 4.4. The intensity of these signals increases as Mo loading increases from 12% in Figure 4.4 (b) to 17% in Figure 4.4 (f). It can be understood that the crystallite size of Mo particles increases beyond 10% loading in Figure 4.4 (a) leading to intense signals corresponding to different phases of Mo particles in Figure 4.4 (b-f). By the forgoing observations, 10% Mo loading seems to be the optimum capacity of this method in order to ensure that the Mo particles are kept small and dispersed thereby avoiding the formation of dense poorly dispersed Mo particles. This is quite interesting as there is a significant enhancement of Mo loading by this method as compared to the previous claims that molydenum oxide is only well dispersed up to 8% loading on the unmodified SBA-15 support [75,76].

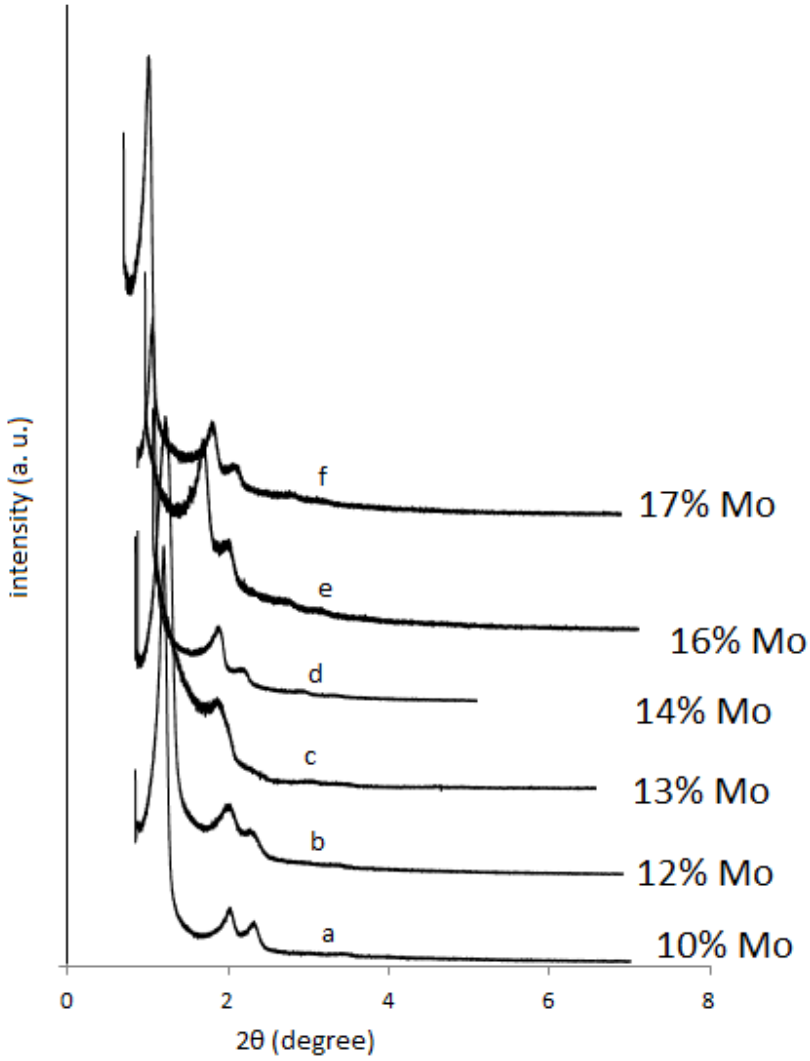

Figure 4.3: Low Angle XRD Patterns of Mo-SBA-15 Catalysts as a Function of Mo loading.

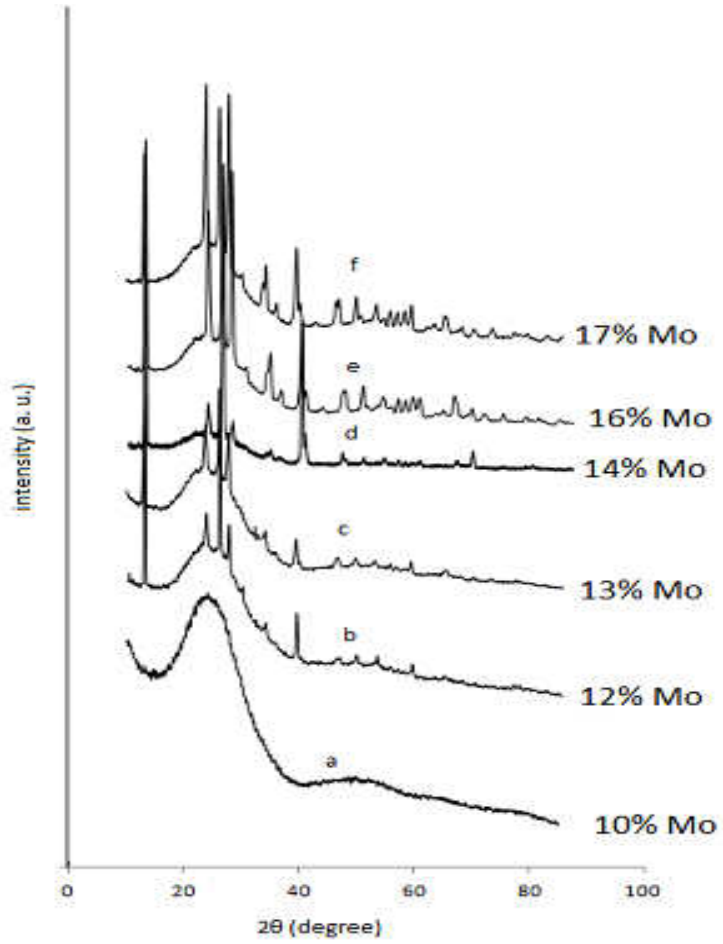

Figure 4.4: Wide Angle XRD Patterns of Mo-SBA-15 Catalysts as a Function of Mo loading.

4.2.2 Sulfide Catalysts

Figure 4.5 compares the low angle diffractograms of the catalyst with 10% Mo and its sulfided form. After sulfidation at 400°C at 10% H_2S/H_2, the low angle diffractions show a slight expansion of the mesopore as we move from Figure 4.5 a to Figure 4.5b. This is obviously due to the transformation of MoO_3 to a bulkier MoS_2 in the mesopores of the silica. Other catalysts show similar trends in the low angle regime after sulfidation. In the wide angle diffractograms, Figure 4.6, the transformation of MoO_3 to MoS_2 is most obvious. Apart from catalyst with 10% Mo which does not show any noticeable peaks, other catalysts show very broad peaks corresponding to MoS_2. However, the intensity of these peaks are, generally, low suggesting that poorly crystallized MoS_2 phases are present.

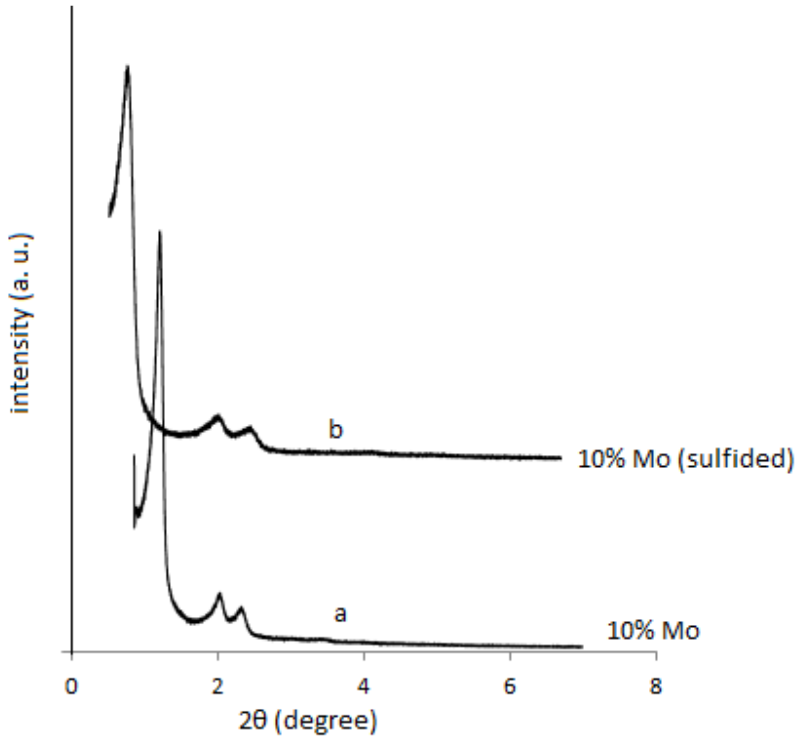

Figure 4.5: Low Angle XRD Patterns of 10% Mo-SBA-15 Catalyst (a) Oxide and (b) Sulfide Forms

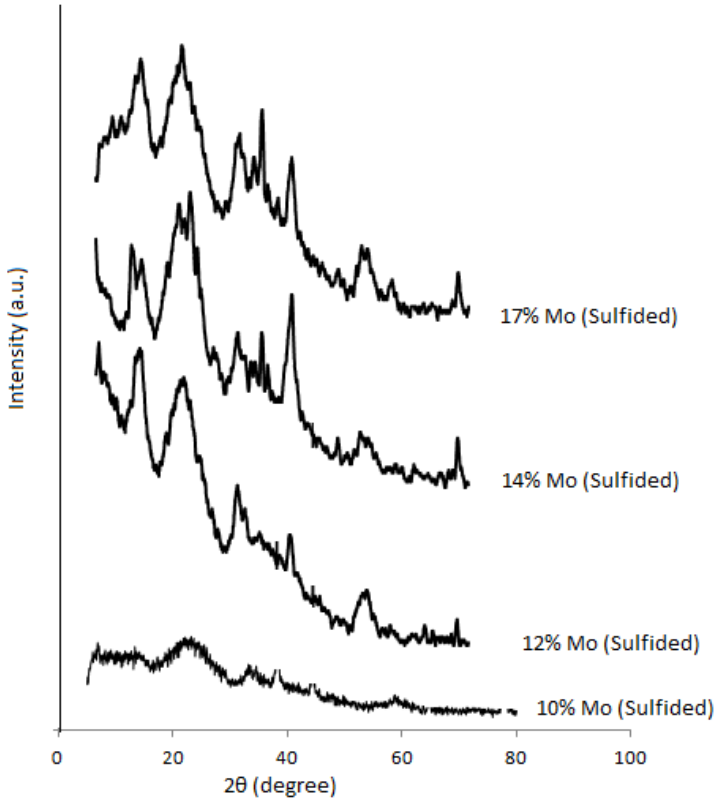

Figure 4.6: Wide angle XRD patterns of MoS_2/SBA-15 Catalysts as a Function of Mo loading.

4.3 DIFFUSE REFLECTANCE UV-VIS SPECTRA

The UV-vis diffuse reflectance spectra of three uncalcined and calcined samples in the range 200nm-600nm are presented in Figure 4.7. In the uncalcined samples, Figure 4.7 (a), two characteristic absorption bands can be observed. The first absorption band that covers from 200-250nm is commonly attributed to the presence of isolated Mo^{6+} species both as mono- and dioxo-molybdenum species [77]. The presence of this band of isolated Mo^{6+} is a first indication of the dispersion of Mo species. This band persists as the amount of loading is increased from 10% to 17%. Still in the uncalcined samples, a second band in the range of 290-340nm is observed. This band is commonly assigned to the octahedral coordinated Mo^{6+} species as found in silicomolybdic acid (SMA) [78]. The formation of SMA on silica has been used as a measure of the dispersion of Mo species on silica support when the Mo content is about 2 weight percent. Sugino eta al, concluded that the high activity of MoO_3/SiO_2 prepared through sol-gel method in the partial oxidation of methane was due to the formation of finely divided Mo particles which consequently encouraged better formation of active agent silicomolybdic acid (SMA) [79]. The interesting thing, here, is that our samples show the presence of SMA even at much higher concentration than the low percentage they claimed in their report. It, therefore, points to the superiority of this synthesis method for SMA to be detected even at much high concentration of 10-17% Mo.

Upon calcinations at 550°C, Figure 4.7(b), the SMA band diminishes for all the samples. This is in agreement with the previous report that SMA is unstable at this temperature decomposing into SiO_2 and MoO_3 [79, 80]. This may mean that by choosing

a milder temperature of calcination or using alternative route for template removal, the dispersion of Mo species on SBA-15 support may be maximized.

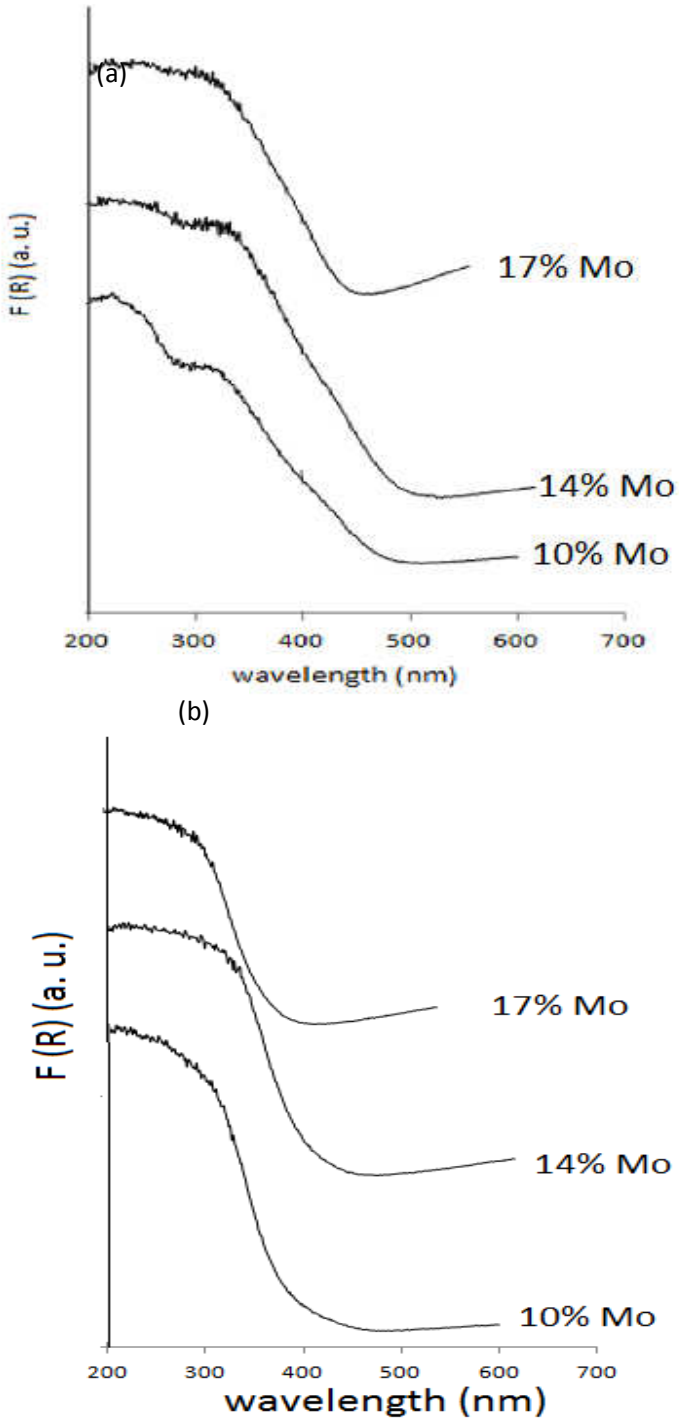

Figure 4.7: DR UV-vis Spectra of Mo-SBA-15 with different Metal loadings for (a) uncalcined (b) calcined Catalysts

4.4 FT-IR SPECTROSCOPY

The IR spectra of uncalcined samples of different Mo loadings and pure SBA-15 are shown in Figure 4.8. The fingerprint region of the IR spectrum of SBA-15 consists of the bands around 795, 1050 and 1630 cm^{-1} in Figure 4.8 (I). These bands have been assigned to Si-O symmetric and asymmetric stretchings in SiO_2 [8]. Introduction of molybdenum into the structures is accompanied with appearance of new bands around 900 and 950 cm^{-1}. The peaks at 900 and 950 cm^{-1} have been assigned to the Si-O-Mo and Mo=O bonds of the silicomolybdic acid (SMA) crystallites respectively [79-81].

Upon calcinations of the samples, Figure 4.9, the appearance of the bands due to SMA diminishes as expected [79, 80] leaving only the characteristic bands for the framework regions of SBA-15. The presence of SMA is reflective of the small nature of MoO_3 particles achieved through this method. [79]. Though the characteristic band for bulk MoO_3 expected at 822cm^{-1} [82] can't be distinguished, however, no conclusion can be made about its exact nature yet as it might have overlapped with band in the framework region of silica at 795 cm^{-1}.

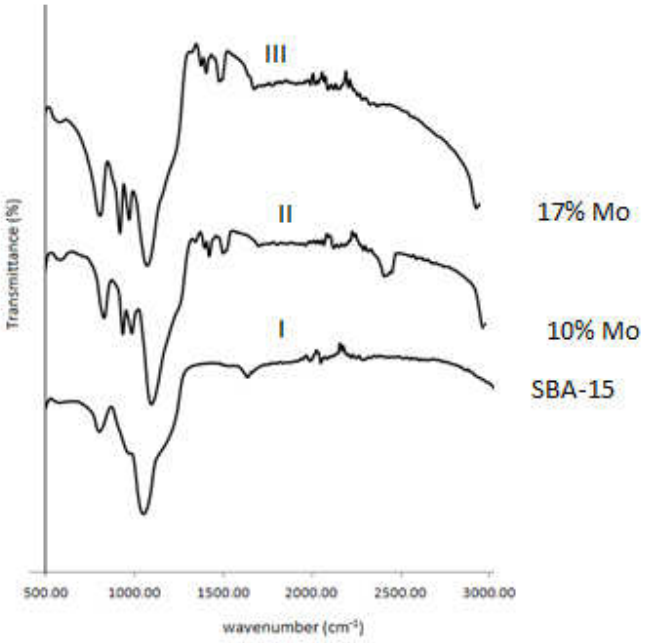

Figure 4.8: FT-IR Spectra of SBA-15 and uncalcined Mo-SBA-15 Catalysts

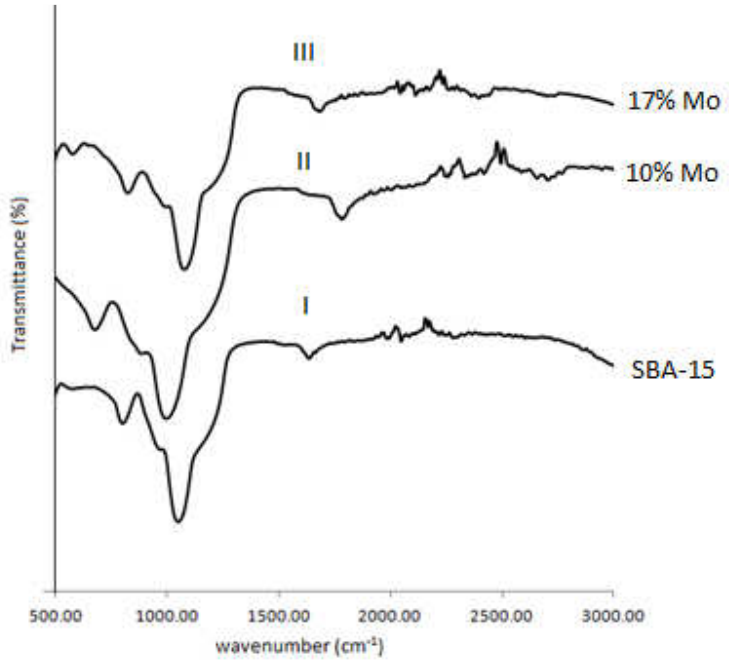

Figure 4.9: FT-IR Spectra of SBA-15 and calcined Mo-SBA-15 Catalysts

4.5 NITROGEN ADSORPTION/DESORPTION ISOTHERMS

Figure 4.10 displays the N_2 adsorption-desorption isotherms acquired at 77K for the sulfided catalysts. The shape of the isotherms is irreversible type-IV, according to the IUPAC classification which includes most of the mesoporous materials. The H1-type hysteresis loop, typical of SBA-15 materials, is also clearly evident, and the sharp steep in the adsorption branch of the isotherms indicates narrow pore size distribution which is typical of a well-ordered mesostructured materials. There is clearly no dramatic change in the shape of the isotherms for all the catalysts as the amount of molybdenum loading is increased from 10% to 16%. This is a confirmation of the fact that this method of co-condensation has been able to deposit up to 16% of molybdenum at convenient sites without affecting the structure of SBA-15 drastically. Low angle XRD diffraction peaks have shown similar results as we saw earlier. However, the starting points of the hysteresis is slightly shifted to higher P/P^0 value when MoS_2 are incorporated, indicating the widening of the mesopores due to deposition of MoS_2 on the pore wall. This trend continues as the molybdenum content of the sulfided catalysts increases from 10% to 16%. The P/P^0 position of the inflexion points is related to the diameter in the mesoporous range.

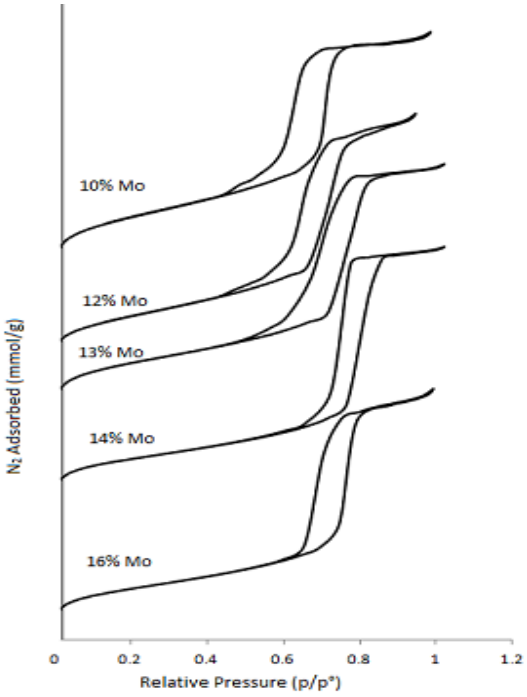

Figure 4.10: N_2 Adsorption-Desorption Isotherms of the Sulfided Mo-SBA-15 Catalysts

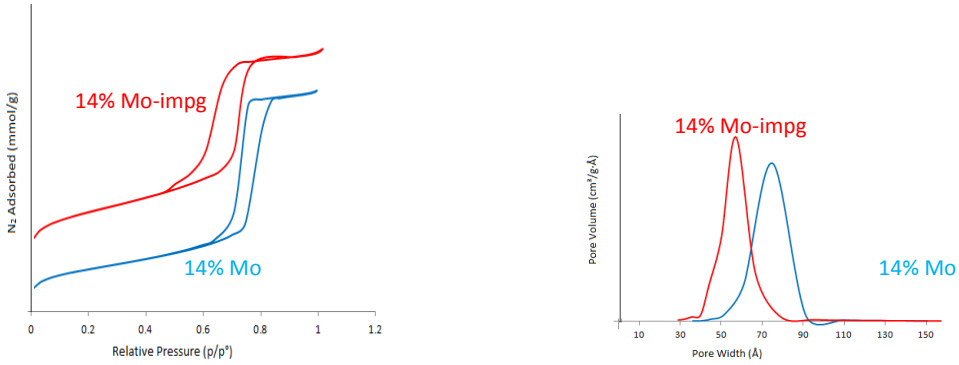

Figure 4.11: N_2 Adsorption-Desorption Isotherms and BJH Pore Size Distribution of the sulfided Mo-SBA-15 Catalysts containing 14% Mo and the Reference impregnated Catalyst containing 14% Mo.

In order to better understand the location of MoS_2 on the structure of SBA-15, the N_2 adsorption-desorption isotherms of the catalyst containing 14% is compared with a reference catalyst containing same amount of molybdenum prepared by impregnation method. Figure 4.11 shows the N_2 isotherms for 14% Mo sulfide catalyst and the impregnated catalyst containing 14% Mo used as a reference. Starting from the reference catalyst, the starting point of the hysteresis slightly shifted to higher P/P^0 value in the catalyst prepared by co-condensation. This means that the co-condensation method deposit the metal exclusively inside the pore (thereby widening the mesopores) while the traditional impregnation method deposit the metal on the surface and as a result do not have much effect on the structure. The BJH pore size distributions of the 14% Mo and the impregnated catalyst used as a reference is also shown in figure 4.11. It can be seen that narrow pore size distribution is obtained in both cases which shift slightly in the case of the catalyst prepared by co-condensation. Other textural properties are shown in table 4.2. The BET surface area shrinks from 406m²/g for the catalyst with 10% Mo to 269m²/g for the catalyst with 16% Mo loading. This is due to the filling of the pore and the coverage of the surface of the support by the molybdenum metal loading. The pore diameter and pore volume also show similar trend.

Table 4.2: Textural Properties of the Sulfided Catalysts

catalysts	S_{BET} (m^2/g)	PD (Å)	PV (cm^3/g)	d_{100} (Å)	Wt (Å)
Mo-SBA-15-10	406	55.2	0.573	86.2	44.3
Mo-SBA-15-12	355	64.9	0.631	83.4	31.4
Mo-SBA-15-13	318	62.8	0.562	96.6	48.7
Mo-SBA-15-14	271	74.2	0.621	87.6	27.0
Mo-SBA-15-16	269	70.8	0.568	74.7	15.4
Mo-SBA-15-14-impg	293	54.1	0.466	89.1	48.8

S_{BET}- surface area calculated by BET method

PD- pore diameter

PV- pore volume

Wt- Wall thickness calculated from XRD experiments and N_2 adsorption analysis (Wt = $\{d_{100}.2/\sqrt{3}\}$ -PD)

4.6 CATALYST ACTIVITY

Table 4.3 shows the final conversion and the yield of each product in the hydrodesulfurization (HDS) of dibenzothiophene (DBT) for the different catalysts used after 3 hours of reaction using 5000ppm DBT at 375°C. The major products of the reaction as identified by GC-MS are cyclohexylbenzene (CHB), biphenyl (BP) and tetrahydrodibenzothiophene (THDBT). Some Bi-cyclic compounds were also identified but their concentrations were too low to be quantified. After 3 hours of reaction, catalyst with 10% Mo reached the highest level of conversion over other catalysts. In all the catalysts the yield of CHB is generally higher than that of the BP. Since it has already been established that BP is usually a product of direct desulfurization of DBT while CHB results from subsequent hydrogenation of partially hydrogenated DBT or BP, the preponderance of CHB over BP is an early hint for the preference of these catalysts for HYD route. Similar observation has been reported elsewhere [83]. The yield of THDBT is generally lowest in the reaction system suggesting that it might be an intermediate.

Table 4.3: Conversion and Product Distributions for HDS of DBT over Mo-SBA-15 Catalysts at 375°C.

Catalysts	%Conversion DBT	% yield of products		
		%CHB	%BP	%THDBT
Mo-SBA-15-10	74.13	53.81	20.31	0.016
Mo-SBA-15-12	62.13	42.76	16.59	2.787
Mo-SBA-15-13	44.08	29.92	13.65	0.507
Mo-SBA-15-14	66.71	39.74	26.49	0.470
Mo-SBA-15-16	68.91	42.13	25.69	1.08
Mo-SBA-15-17	68.37	39.53	27.52	1.314
Mo-SBA-15-14-impg	57.79	35.69	20.92	1.172

In order to gain more insights into the product distribution of the reaction, the percentage conversion of DBT were plotted against the product yields for all the catalysts. Figures 4.12-4.14 display the products selectivity versus the conversion of DBT at 325, 350 and 375°C for Mo-SBA-15-10, the best catalyst with 74% DBT conversions. Biphenyl as a product of DDS route is related to the direct scission of the C-S bond in the DBT. The plots show a good yield of BP which reaches a constant value towards the end of the reaction. This may mean that BP is involved in further reactions to form other products although the rate of its subsequent reactions may be too slow to make any significant contributions to the global HDS of DBT. It has been reported that the rate of BP hydrogenation is significantly low in the presence of DBT, because DBT successfully competes with BP for the hydrogenation sites of the catalysts [39, 59, 65]. Furthermore, CHB which is understood as a product from partial hydrogenation of THDBT through HYD route is the dominant product. On the other hand, the product distribution of THDBT suggests it is the least stable product. The distribution goes through a maximum and gradually decays to zero. Thus, THDBT is considered as an intermediate that participates in a further reaction to produce CHB. This trend is seen for all the seven catalysts used during the reaction at different reaction temperatures used. The above results indicate that HDS of DBT over these catalysts occurs through a greater contribution from hydrogenation (HYD) route than direct desulfurization route (DDS) route. On the basis of the above product analysis, scheme 4.1 was proposed for the HDS of DBT over these catalysts.

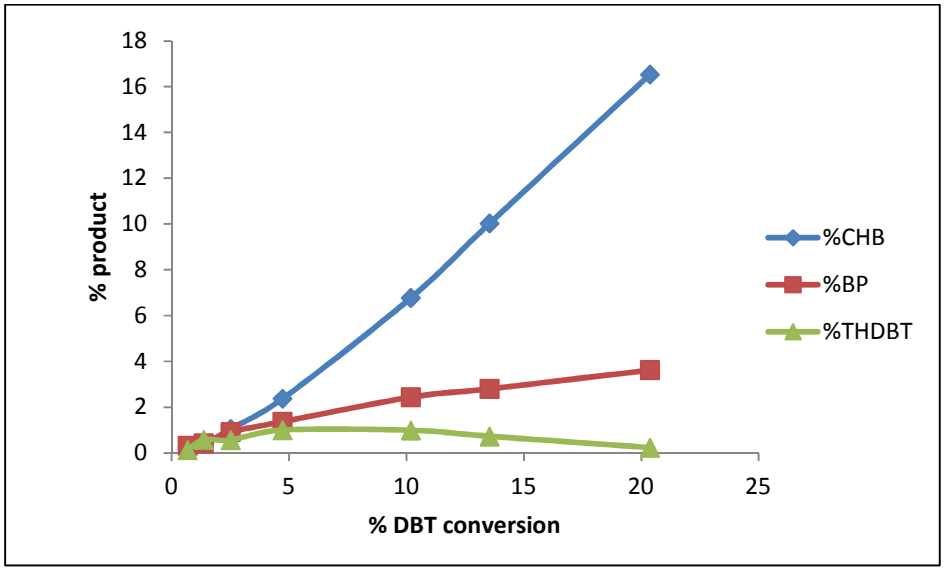

Figure 4.12: Product Selectivity vs. Conversion of DBT at 325°C for Mo-SBA-15-10

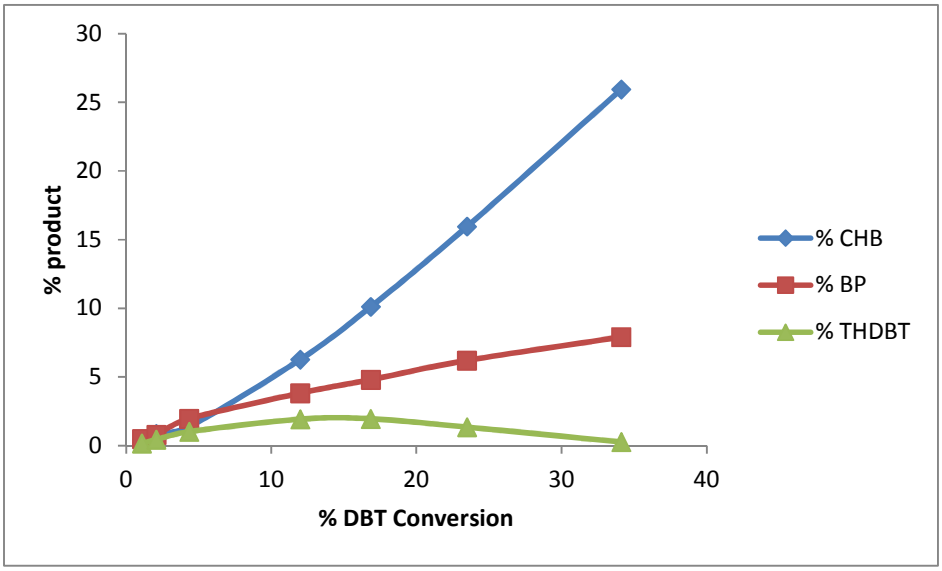

Figure 4.13: Product Selectivity vs. Conversion of DBT at 350°C for Mo-SBA-15-10

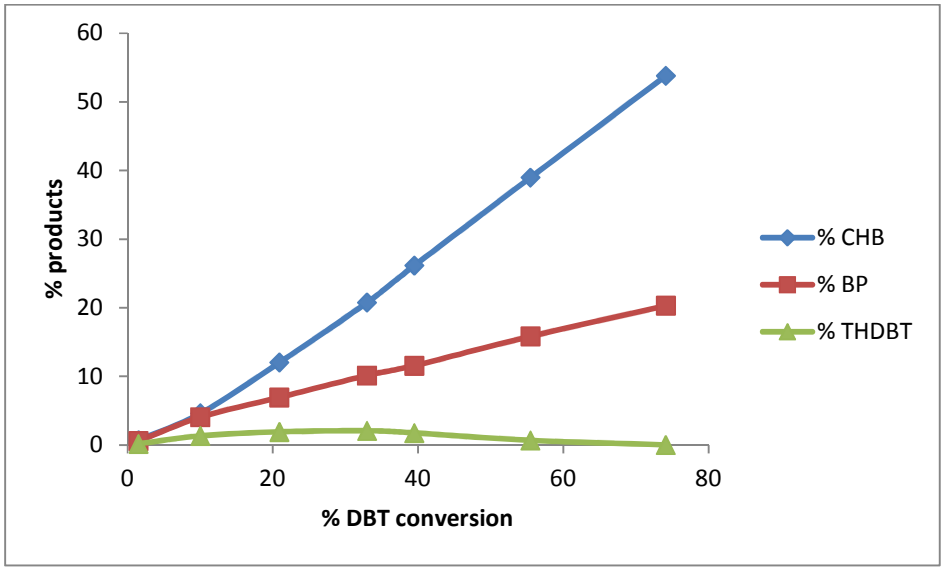

Figure 4.14: Product Selectivity vs. Conversion of DBT at 375°C for Mo-SBA-15-10

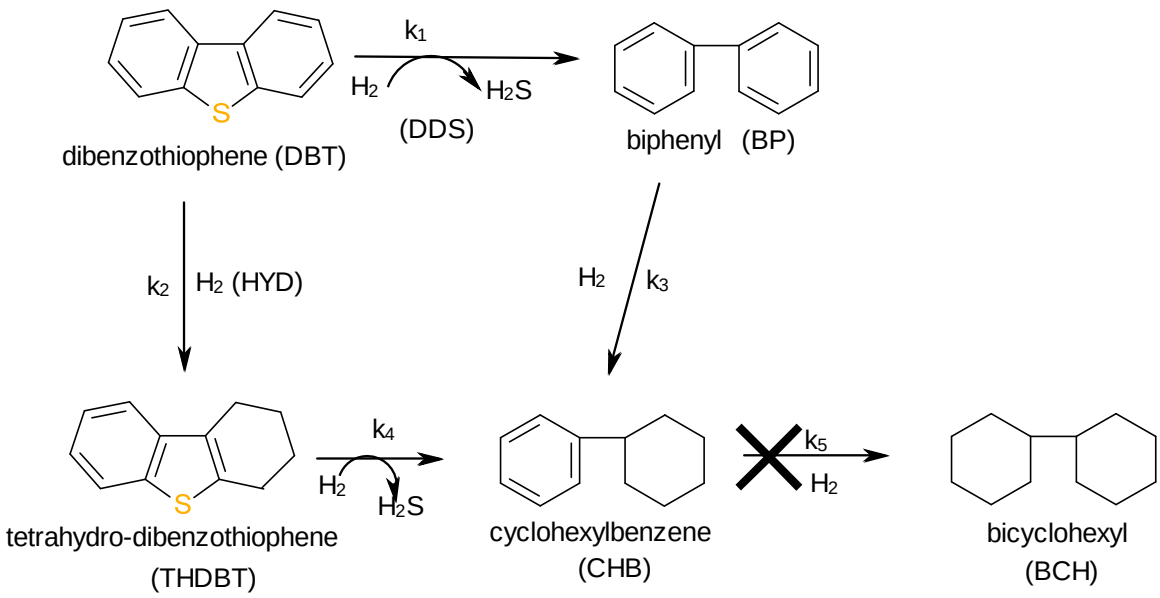

Scheme 4.1: Proposed Reaction Network for the HDS of DBT

4.7 KINETIC TREATMENT

In order to verify the proposed mechanism, the kinetic equations that fit the experimental data obtained in HDS of DBT based on Langmuir-Hinshelwood (L-H) type equation with two kinds of catalytic active sites [85, 86] were developed.

Accordingly, the overall rate can be expressed by two parts:

$$R_{DDS} = \frac{k_1 K_1 C_{DBT}}{1 + K_1 C_{DBT} + \cdots} \qquad (1)$$

$$R_{HYD} = \frac{k_2 K_2 C_{DBT}}{1 + K_1 C_{DBT} + \cdots} \qquad (2)$$

Here, R_{DDS} and R_{HYD} are the rate of direct desulfurization (DDS) and the rate of hydrogenation (HYD) of DBT, respectively. K_1, k_1 and K_2, k_2 are the equilibrium adsorption constants of DBT over the catalytic active sites and the reaction rate constants for DDS and HYD, respectively. C_{DBT} is the concentration of DBT at a given reaction time.

Under the reaction conditions used, the rate equations (1and 2) reduce to pseudo-first order equations where the overall rate, R_{total} can be taken as the sum of the rate of direct desulfurization (DDS) and the rate of hydrogenation (HYD):

$$R_{total} = (k_1 K_1 + k_2 K_2) C_{DBT} \qquad (3)$$

$$R_{total} = k_0 C_{DBT} \qquad (4)$$

Where $k_0 = (k_1 K_1 + k_2 K_2)$ is taken as the apparent rate constant of the DBT conversion. By considering every component of the reaction network, the material balance equations (of a batch reactor) of all the components of the reaction network in **scheme 4.1** can be written as follow:

$$\frac{dC_{DBT}}{dt} = k_0 C_{DBT} \qquad (5)$$

$$\frac{dC_{BP}}{dt} = k_1 C_{DBT} - k_3 C_{BP} \quad (6)$$

$$\frac{dC_{THDBT}}{dt} = k_2 C_{DBT} - k_4 C_{THDBT} \quad (7)$$

Where k_1, k_2, k_3 and k_4 are the apparent rate constants of the respective steps in the reaction network in scheme 4.1. Further treatments of these equations (5-7) lead to the following expressions:

$$C_{DBT} = C_{DBT}^0 e^{-k_0 t} \quad (8)$$

$$C_{BP} = C_{BP}^0 e^{-k_3 t} + \frac{C_{DBT}^0 k_1}{k_3 - k_0}[\, e^{-k_0 t} - e^{-k_3 t}] \quad (9)$$

$$C_{THDBT} = C_{THDBT}^0 e^{-k_4 t} + \frac{C_{DBT}^0 k_2}{k_4 - k_0}[e^{-k_0 t} - e^{-k_4 t}] \quad (10)$$

WhereC_{DBT}^0, C_{BP}^0, C_{THDBT}^0 are the concentrations at reaction time t=0 of the DBT, BP, and THDBT respectively.

Considering the experimental conditions used in this study, the following assumptions have been made:

1. The hydrogen concentration remains constant throughout the reaction since it was fed in excess.
2. HDS of individual sulfur compounds follow pseudo-first order kinetics [83].
3. The contribution of the hydrogenation pathway of BP to CHB was found negligible as previously reported [39, 59, 65,]. Hence, calculated K_3 was found to be zero.
4. The inhibition effect of the products of HDS of DBT is considered negligible [84]. The effect of $_{H2}$S was neutralized by addition of Cu powder to the reaction mixture.

4.7.1 COMPUTATIONAL ANALYSIS

Computational analyses were carried out using Mathematica 5.0 to fit the experimental data with Langmuir-Hinshelwood (L-H) equations. Kinetic parameters were generated at a correlation factor of greater than 95% between experimental and calculated data. Figures 4.15-4.17 show the comparism between experimental and calculated concentrations for the reaction at 375°C over catalyst with 10% Mo. Interestingly, in all the fittings, we obtained very good correlation between the experimental and theoritical data. For the DBT curve, figure 4.15, the concentration of DBT decreases exponentionally with reaction time in accordance with kientic of pusedo-first order conversion. Figures 4.16-4 and 4.17 also display the fitting curves for the other products. Although, in all, there are good agreements between experimental and the calculated data, a slight deviation is noticed for the THDBT curve. This deviation originates from rather inaccurate measurement of low concentrations of THDBT by GC-MS. Hence, using a modified approach whereby the total products from HYD route (including intermediates) are considered, a more useful curve can be obtained.

Thus, the mass balance for the hydrogenation route is as follows:

$$C_{DBT}(HYD) = C_{THDBT} + C_{CHB} \qquad (11)$$

And the rate of hydrogenation from equation (2) becomes:

$$R_{HYD} = k_2 C_{DBT} \qquad (12)$$

Upon integration, this equation becomes:

$$C_{HYD} = \frac{k_2}{K_0} C^0_{DBT}(1 - e^{-k_0 t}) + C^0_{THDBT+CHB} \quad (13)$$

By fitting the experimental data on total hydrogenated products with equation (13) as depicted in Figure 4.18, a much more precise estimate of k_2 was obtained.

Thus, confirming the previous claims that this model is satisfactory for HDS of DBT [84].

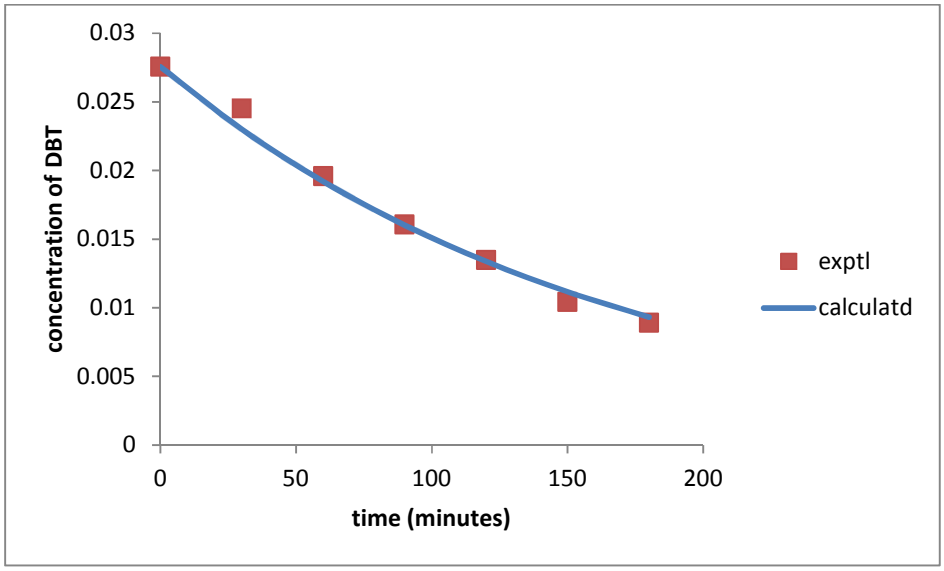

Figure 4.15: Concentration of DBT as a Function of Reaction Time at 375°C

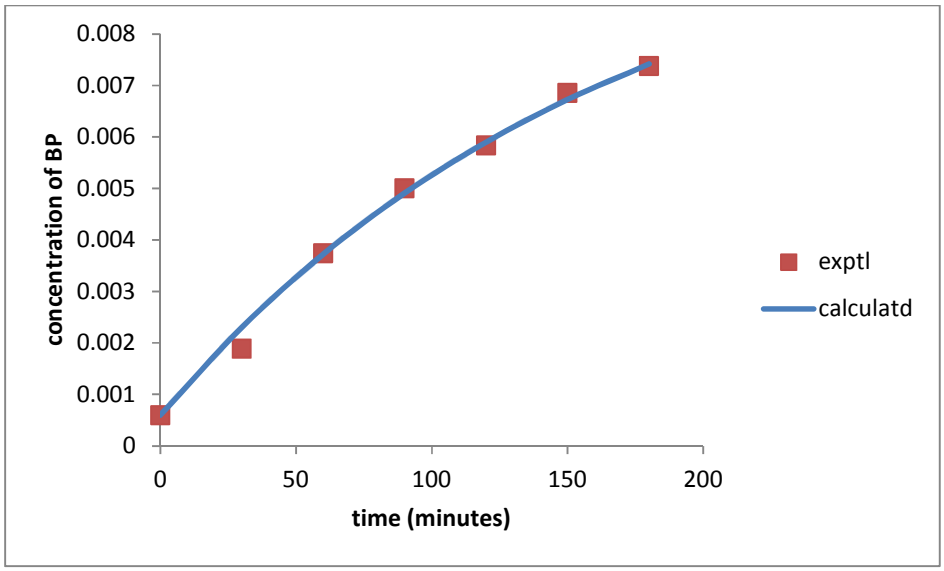

Figure 4.16: Concentration of BP as a Function of Reaction Time at 375°C

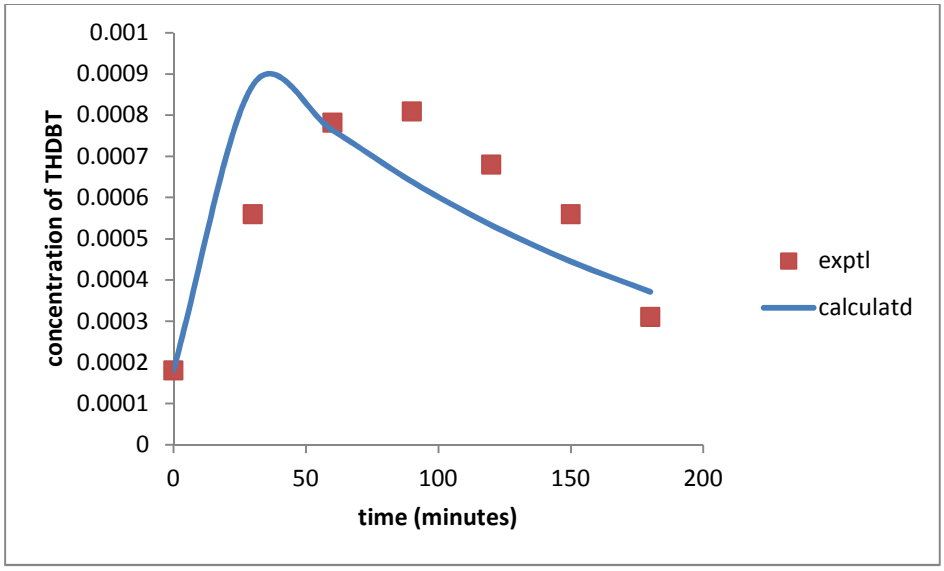

Figure 4.17: Concentration of THDBT as a Function of Reaction Time at 375°C

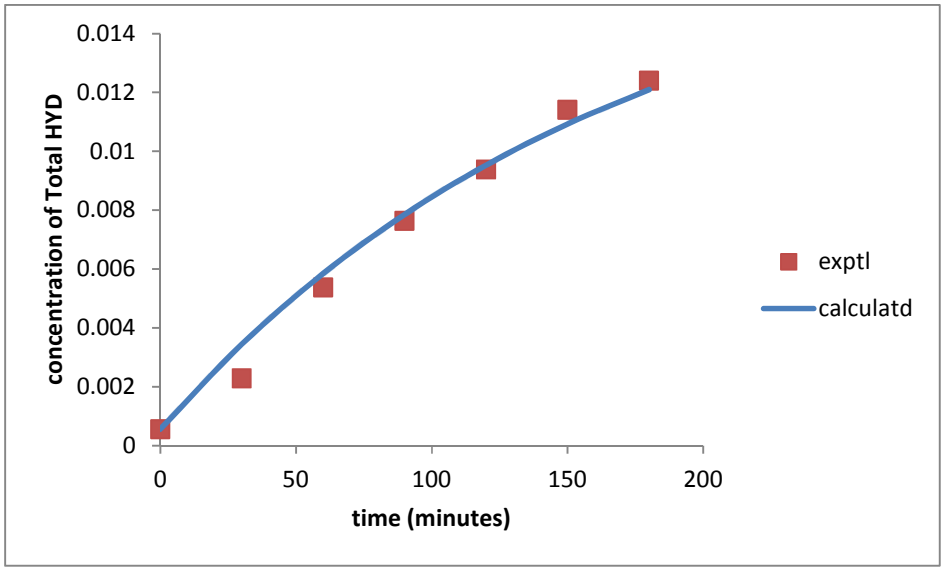

Figure 4.18: Concentration of Total HYD as a Function of Reaction Time at 375°C

Meanwhile in order to evaluate the relative contribution and selectivity of each of the two pathways-DDS and HYD-the kinetic parameters for various catalyst have been compared in table 4.3. In all the catalysts, the rate constant for the hydrogenation route, k_2 is higher than that of DDS route, K_1. Thus, the selectivity factor k_2/k_1 is consistently higher than 1 with the highest value being ~4 for the catalyst with 10% Mo on the silica support. This reveals that the transformation of DBT over these catalysts is highly favored by hydrogenation route in accordance with previous report that SiO_2 enhances the contribution of HYD pathway [83]. The highest selectivity factor of ~4 obtained for the catalyst with 10% loading corroborates the characterization results that the Mo species on the SBA-15 support are small and well dispersed. This can further be explained on the rim/edge model put forward by Chianelli and Daage that for large molecules like DBT, hydrogenation reaction occurs predominantly at the rim site while sulfur hydrogenolysis occurs at the edge sites [86]. In our own case, by having small particles of the catalysts well dispersed on the SBA-15 leads to the availability of more rim sites than edge site. Thus accounting for better hydrogenation preferences of these catalysts.

The kinetic parameters estimated at different temperatures for all the catalysts were used to obtain the apparent activation energy (Ea) and the pre-exponential factor, A, for the HDS of DBT. The activation parameters are shown in table 4.4. The lowest activation energy of 109kJ/mole is obtained for catalyst with 10.35% Mo loading. This is about 2 times smaller than the highest activation energy obtained for the impregnated catalyst containing about 14% Mo which was used as a reference. Also catalyst with 14% Mo synthesized through our method shows greater activity in comparism with impregnated catalyst containing the same amount of Mo. Thus, we could say that all the catalysts

synthesized through our method show greater activity probably because of better dispersion of the active phase in comparism with conventional impregnated catalysts.

Table 4.4: Overall and Individual Apparent Rate Constants for the HDS of DBT at 325, 350°C and 375°C.

		rate constants $x10^{-3}$					
Catalyst	T (°C)	k_0 (min^{-1})	k_1 (min^{-1})	k_2 (min^{-1})	k_4 (min^{-1})	k_{HYD} (min^{-1})	k_2/k_1
	325	0.92	0.18	0.75	98.79	0.75	4.22
	350	1.70	0.43	1.27	89.69	1.28	2.95
Mo-SBA-15-10	375	5.05	1.46	3.58	165.33	3.68	2.45
	325	0.43	0.15	0.28	15.80	0.28	1.83
	350	1.06	0.32	0.74	31.23	0.74	2.30
Mo-SBA-15-12	375	3.46	0.93	2.53	59.50	2.57	2.73
	325	0.40	0.11	0.29	16.24	0.29	2.53
	350	1.42	0.41	1.01	37.86	1.02	2.49
Mo-SBA-15-13	375	3.57	1.10	2.47	42.81	2.44	2.24
	325	0.27	0.11	0.16	5.87	0.16	1.40
	350	0.96	0.35	0.61	22.14	0.61	1.73
Mo-SBA-15-14	375	5.69	2.27	3.42	103.09	3.39	1.51
	325	0.28	0.09	0.19	13.87	0.19	2.08
	350	0.86	0.31	0.54	30.07	0.54	1.72
Mo-SBA-15-16	375	6.03	2.25	3.78	100.80	3.81	1.68
	325	0.49	0.18	0.31	19.64	0.32	1.79
	350	1.28	0.35	0.93	42.72	0.94	2.66
Mo-SBA-15-17	375	6.95	2.85	4.10	28.48	4.05	1.43
	325	1.70	0.67	1.04	391.74	1.04	1.55
	350	2.19	0.81	1.39	306.46	1.40	1.73
Mo-SBA-15-14-impg	375	3.26	1.29	1.97	105.86	2.03	1.53

Table 4.5: Apparent Activation Parameters for the HDS of DBT.

Catalyst	Ea	A
	(kJ/mole)	(min^{-1})
Mo-SBA-15-10	109	2.78×10^{6}
Mo-SBA-15-12	135	2.37×10^{8}
Mo-SBA-15-13	142	9.92×10^{8}
Mo-SBA-15-14	195	2.71×10^{13}
Mo-SBA-15-16	197	3.98×10^{13}
Mo-SBA-15-17	170	3.19×10^{11}
Mo-SBA-15-14-impg	210	5.47×10^{14}

Figure 4.19 compares the activities of these catalysts per gram Mo in the Hydrodesulfurization (HDS) of DBT at 375°C. The highest value of apparent rate constant per gram of Mo is observed for the catalyst with 10% Mo as previously noted. This catalyst is about two times more active than the impregnated catalyst with greater amount (14%) of Mo active phase.

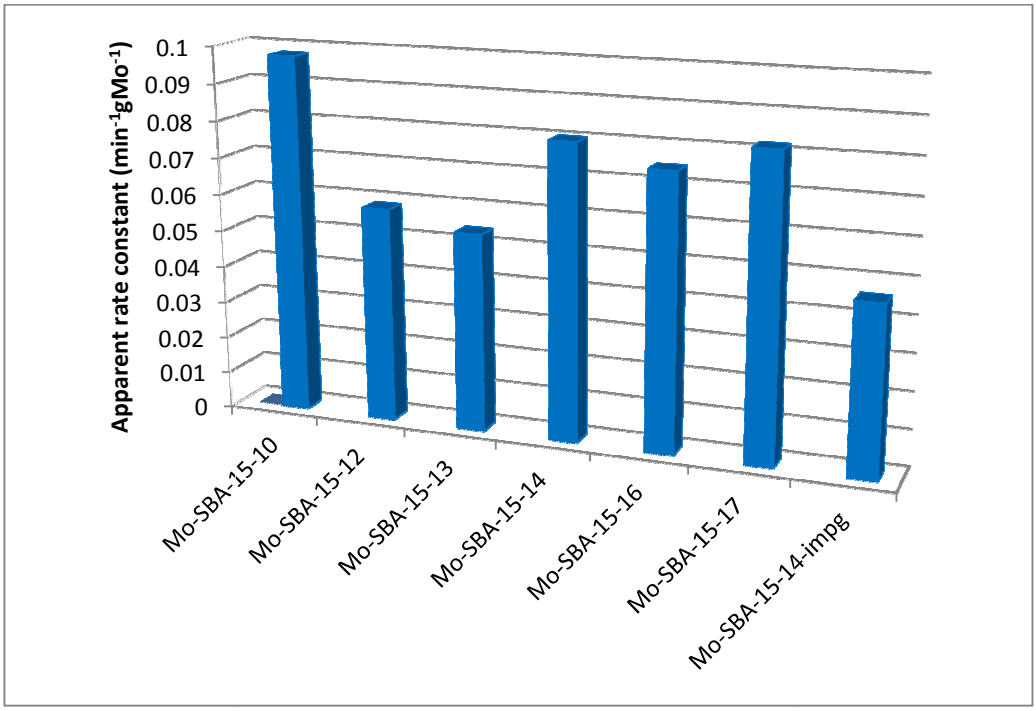

Figure 4.19: Intrinsic Catalytic Activity in the HDS of DBT at 375°C per gram of Mo for supported MoS_2 Catalysts.

CHAPTER 5

CONCLUSIONS AND RECOMMENDATIONS

5.1 CONCLUSIONS

Using co-condensation method, Mo-SBA-15 materials containing varying amount of molybdenum loading up to 17% wt have been synthesized from acidic solution of its precursors. The following are the summary of our investigations:

1. The effect of acid concentration on the incorporation efficiency of the metal into the silica structure was investigated. It was noted that higher acid concentration limits the incorporation of the metal into silica matrix. This is consistent with previous reports [72-74].
2. By manipulation of the synthesis parameters such as pH, stirring rate and time, ripening and aging time, the interaction between silica and molybdenum metal was enhanced leading to the formation of SMA as confirmed by our characterization method. The formation of SMA on silica support has only been reported at low molybdenum content of about 2% on silica and it is understood to be as a result of dispersion of Mo particles on the support [8]. We, hereby, report SMA at much higher concentration of above 10% weight of active metal. The

detection of SMA in the as-synthesized materials even after increased loading is indicative of the improved interaction between the silica support and molybdenum active phase and hence a proof of the dispersion of active phase.

3. Low angle XRD reveals that the structural integrity of the ordered mesoporous materials is still highly preserved after increased loading. As suggested by our various characterization techniques, the catalyst with 10% Mo loading shows the best dispersion of Mo active phase. This is quite interesting as previous efforts reached best dispersion of Mo active phase only at 8% loading on unmodified SBA-15 [75, 76].
4. The activity of the catalysts in the overall HDS reactions is good with highest being for the catalyst with 10% Mo. All the catalysts show superior activity in comparison to the impregnated catalyst used as a reference.
5. Kinetic analyses of the reaction data showed that all the catalysts have selectivity for hydrogenation pathway in the HDS of DBT. This may mean some promises in the HDS of alkyl DBTs as their HDS is known to proceed more easily through hydrogenation route.

5.2 RECOMMENDATIONS

A few recommendations will be made here concerning the improvement of the catalysts and prospective applications for other reactions. Future work on these catalysts may include the following:

1. Incorporation of promoter: Conventional hydrodesulfurization catalysts are usually promoted with Ni or Co depending on the desired outcome. Suitably

promoted catalysts are known to give better performance than their unpromoted counterparts. The choice of usually depends on the nature of feed and the desired reaction. Promotion of this catalyst with Co may improve its direct desulfurization functionalities [8].

2. Use of the catalyst on more refractory alkyl DBT in the real feed: Hydrodesulfurization of alkyl DBTs are known to favor hydrogenation pathway. Since this catalyst show stronger preference for hydrogenation than direct desulfurization, it may prove effective in the HDS of sterically hindered sulfur compounds.
3. The reusability of these catalysts: Our investigations as discussed above show evidence of the active metal deposited majorly in the pores of the silica. This means that reusability of these catalyst may be enhanced as the active metal are not easily leached inside the pores after several reaction runs.
4. TEM Micrographs: Future studies should also include the transmission electron microscopy in order to ascertain correctly the size of the particles, their stacking height and the distribution.

REFERENCES

[1] M. Breysse, G. Djega-Mariadassou, S. Pessayre, C. Geantet, M. Vrinat, G. Perot, M. Lemaire, Deep desulfurization: reactions, catalysts and technological challenges, Catal. Today 84 (2003) 129.

[2] I.V. Babich, J.A. Moulijn, Science and technology of novel processes for deep desulfurization of oil refinery streams: a review, Fuel 82 (2003) 607.

[3] (a) C. Song, An overview of new approaches to deep desulfurization for ultra-clean gasoline, diesel fuel and jet fuel, Catal. Today 86 (2003) 211-263.
(b) C. Song, X. Ma, New design approaches to ultra-clean diesel fuels by deep desulfurization and deep dearomatization, Appl. Catal. B: Environ. 41 (2003) 207.

[4] I. Vergov, I. Shishkova, Catalyst advances promote production of near zero sulphur diesel, Petrol. Coal 51 (2009) 136–139.

[5] Sajkowski, D.J., & Oyama, S.T., Catalytic hydrotreating by molybdenum carbide and nitride, (1996). Appl. Catal. A 134, 339-349.

[6] Oyama, S.T. Novel catalysts for advanced hydroprocessing: transition metal phosphides, (2003). J. Catal., 216, 343.

[7] Whitehurst, D.D., Isoda, T., & Mochida, I., Present state of the art and future challenges in the hydrodesulfurization of polyaromatic sulfur compounds (1998). Adv. Catal. 42, 345-471.

[8] A. Stanislaus, A. Marafi, M. S. Rana, Recent advances in the science and technology of ultra low sulfur diesel (ULSD) production, Catalysis Today 153 (2010) 1-68.

[9] NEBuLA-20 (introduced in market 2004): http://www.albemarle.com/TDS/HPC/NEBULA-20 The%20 next step into deep space.pdf;
(b) Y. Gochi, C. Ornelas, F. Paraguay, S. Fuentes, L. Alvarez, J.L. Rico, G. Alonso-Nunez, Effect of sulfidation on Mo–W–Ni trimetallic catalysts in the HDS of DBT, Catal. Today 107–108 (2005) 531–536.

[10] D. Krenzke, M. Zehender, SMART catalyst system effective in ULSDapplications, Hydrocarbon Asia 12 (2002) 44–48.

[11] Topsoe hydrotreating catalysts: http://www.topsoe.com/products/CatalystPortfolio.aspx.

[12] H. Topsøe, B. Hinnemann, J.K. Nørskov, J.V. Lauritsen, F. Besenbacher, P.L. Hansen, G. Hytoft, R.G. Egeberg, K.G. Knudsen, The role of reaction Path ways and support interactions in the development of high activity Hydrotreating catalysts, Catal. Today 107–108 (2005) 12.

[13] P. Rayo, M.S. Rana, J. Ramirez, J. Ancheyta, A. Aguilar-Elguezabal, Effect of the preparation method on the structural stability and hydrodesulfurization activity of NiMo/SBA-15 catalysts, Catal. Today 130 (2008) 283–291.

[14] M. Breysse, P. Afanasiev, C. Geantet, M. Vrinat, Overview of support effects in hydrotreating catalysts, Catal. Today 86 (2003) 5–16.

[15] M. Breysse, C. Geantet, P. Afanasiev, J. Blanchard, M. Vrinat, Recent studies on the preparation, activation and design of active phases and supports of hydrotreating catalysts, Catal. Today 130 (2008) 3.

[16] E.J.M. Hensen, P.J. Kooyman, Y. van der Meer, A.M. van der Kraan, V.H.J. de Beer, J.A.R. van Veen, R.A. van Santen, The relation between supports of hydrotreating catalysts, Catal. Today 130 (2008) 3.

[17] E.J.M. Hensen, V.H.J. de Beer, J.A.R. van Veen, R.A. van Santen, A refinement on the notion of type I and 11 (Co) MoS phases in hydro- treating catalysts, Catal. Lett. 84 (2002) 1–2.

[18] K. P. de Jonge (editor), Synthesis of solid catalysts, Wiley publication, pp. 301-328.

[19] A. Corma, A. Martinez, V. Martinez-Soria, J.B. Montón, Hydrocracking of vacuum gasoil on the novel mesoporous MCM-41 aluminosilicate catalyst, J. Catal. 153 (1995) 25–31.

[20] A. Corma, M.S. Grande, V. Gonzalez-Alfaro, A.V. Orchilles, Cracking activity and hydrothermal stability of MCM-41 and its comparison with amorphous silica–alumina and a USY zeolite, J. Catal. 159 (1996) 375–382.

[21] T. Klimova, M. Calderon, J. Ramirez, Ni and Mo interaction with Al-containing MCM-41 support and its effect on the catalytic behavior in DBT hydrodesulfurization, Appl. Catal. A: Gen. 240 (2003) 29-40.

[22] A. Wang, Y. Wang, T. Kabe, Y. Chen, A. Ishihara, W. Quian, P. Yao, Hydrodesulfurization of dibenzothiophene over siliceous MCM-41-supported catalysts. II. sulfided Ni–Mo catalysts, J. Catal. 210 (2002) 319–327.

[23] M. Nagai, Appl., Transition-metal nitrides for hydrotreating catalyst-Synthesis, surface properties, and reactivities, Catal. A: Gen. 322 (2007) 178-190.

[24] R.R. Bharvani, R.S. Henderson, Revamp your hydrotreater for deep desulfurization: clean fuels, Hydrocarb. Process. 81 (2002) 61–64.

[25] T. Fujikawa, H. Kimura, K. Kiriyama, K. Hagiwara, Development of ultra-deep HDS catalyst for production of clean diesel fuels, Catal. Today 111 (2006) 188–193.

[26] Y. Okamoto, M. Breysse, G. Murali Dhar, C. Song, Effects of support in hydrotreating catalysis for ultra-clean fuels, Catal. Today 86 (2003) 1–288.

[27] X. Ma, L. Sun, C. Song, A new approach to deep desulfurization of gasoline, diesel fuel and jet fuel by selective adsorption for ultra-clean fuels and for fuel cell applications, Catal. Today 77 (2002) 107.

[28] S. Torrisi, The challenging chemistry of ultra-low sulfur diesel. Process Technology, Catalysis, World Refining. December, 2002 (http://www.shell.com/static/criterion-gb/downloads/pdf/trade pub reprints/wr 1201reprinttorrisi ulsd.pdf).

[29] R. Shafi, G.J. Hutchings, Hydrodesulfurization of hindered dibenzothiophenes: an overview, Catal. Today 59 (2000) 423–442.

[30] T. Kabe, A. Ishihara, Q. Zang, Deep desulfurization of light oil. Part 2: hydrodesulfurization of dibenzothiophene, 4-methyldibenzothiophene and 4,6-dimethyldibenzothiophene, Appl. Catal. A 97 (1993) L1–L9.

[31] T.C. Ho, Deep HDS of diesel fuel: chemistry, Catal. Today 98 (2004) 3–18.

[32] H. Schulz, W. Bohringer, P. Waller, F. Ousmanov, Gas oil deep hydrodesulfurization: refractory compounds and retarded kinetics, Catal. Today 49 (1999) 87–97.

[33] M. Houalla, D. Broderick, V.H.J. de Beer, B.C. Gates, H. Kwart, Hydrodesulfurization of dibenzothiophene and related compounds catalyzed by sulfided CoO–MoO3/_-Al2O3: effects of reactant structure on reactivity, Am. Chem. Soc. Prep. Div. Petrol. Chem. 22 (1977) 941.

[34] V. Meille, E. Schulz, M. Lemaire, M. Vrinat, Hydrodesulfurization of alkyldibenzothiophenes over a NiMo/Al2O3 catalyst: kinetics and mechanism, J. Catal. 170 (1997) 29–36.

[35] F. Bataille, J.L. Lenibcrton, P. Michanct, G. Perot, M. Vrinai, M. Lemaire, E. Schulz, M. Breysse, S. Kaszlelan, Alkyldibenzothiophenes hydrodesulfurization-promoter effect, reactivity, and reaction mechanism, J. Catal. 191 (2000) 409–422.

[36] M. Macaud, A. Milenkovic, E. Schulz, M. Lemaire, M. Vrinat, Hydrodesulfurization of alkyldibenzothiophenes: evidence of highly unreactive aromatic sulfur compounds, J. Catal 193 (2000) 255–263.

[37] M. J. Girgis, B.C. Gates, Reactivities, reaction networks and kinetics in high pressure catalytic hydroprocessing, Ind. Eng. Chem. Res. 30 (1991) 2021–2058.

[38] B.C. Gates, H. Topsoe, Reactivities in deep catalytic hydrodesulfurization: challenges, opportunities, and the importance of 4-methyldibenzothiophene and 4,6 dimethyldibenzothiophene, Polyhedron 16 (1997) 3213–3217.

[39] P. Michaud, J.L. Lemberton, G. Perot, Hydrodesulfurization of dibenzothiophene and 4,6-dimethyldibenzothiophene: effect of an acid component on the activity of a sulfided NiMo on alumina catalyst, Appl. Catal. A: Gen. 169 (1998) 343–353.

[40] Topsoe, H., Clausen, B.S., & Massoth, F.E. (1996). Hydrotreating Catslysis Science and Technology, In (Anderson, J.R., & Boudart, M., Eds.), Vol. 11, pp. 65-69. Springer, New York.

[41] Candia, R., Sorensen, O., Villadsen, J., Topsoe, N., Clausen, B.S., & Topsoe, H. (1984). *Bull. Soc. Chim. Belg. 93,* 763.

[42] Y. Okamoto, K. Hioka, K. Arakawa, T. Fujikawa, T. Ebihara, T. Kubota, Effect of sulfidation atmosphere on the hydrodesulfurization activity of SiO_2-supported Co–Mo sulfide catalysts: local structure and intrinsic activity of the active sites, J. Catal. 268 (2009) 49–59.

[43] Y. Okamoto a, A. Kato, N. Usman a, T. Rinaldi, H. Fujikawa, I. Koshika, T. Hiromitsu, Kubota, Effect of sulfidation temperature on the intrinsic activity of Co–MoS2 and Co–WS2 hydrodesulfurization catalysts, J. Catal. 265 (2009) 216–228.

[44] B. Shen, H. Li, W. Zhang, Y. Zhao, Z. Zhang, X. Wang, S. Shen, A novel composite support for hydrotreating catalyst aimed at ultra-clean fuels, Catal. Today 106 (2005) 206–210.

[45] M. J. Vissenberg, Y. van der Meer, E.J.M. Hensen, V.R.J. de Beer, A.M. van der kraan, R.A. van Santen, J.A.R. van veen, The effect of support interaction on the sulfidability of Al2O3 and TiO2 supported CoW and NiW hydrodesulfurization catalysts, J. Catal. 198 (2001) 151–163.

[46] J. P. R. Vissers, B. Scheffer, J.H.J. de Beer, J.A. Moulijh, R. Prins, Effect of the support on the structure of Mo-based hydrodesulfurization catalysts activated carbon versus alumina, J. Catal. 105 (1987) 277-284.

[47] R. G. Lehveld, A.J. van Dillen, J.W. Geus, D.C. Komgsberger, A Mo–K edge XAFS study of the metal sulfide–support interaction in (Co)Mo supported alumina and titania catalysts, J. Catal. 165 (1997) 184–196.

[48] M. Breysse, P. Afanasiev, C. Geantet, M. Vrinat, Overview of support effects in hydrotreating catalysts, Catal. Today 86 (2003) 5–16.

[49] P. Rayo, J. Ramirez, M.S. Rana, J. Ancheyta, A. Aguilar-Elguezabal, Effect of the incorporation of Al, Ti, and Zr on the cracking and hydrodesulfurization activity of NiMo/SBA-15 catalysts, Ind. Eng. Chem. Res. 48 (2009) 1242–1248.

[50] A. Carati, G. Ferraris, M. Guidotti, G. Moretti, R. Psaro, C. Rizzo, Preparation and characterization of mesoporous silica–alumina and silica titania with a narrow pore size distribution, Catal. Today 77 (2003) 315–323.

[51] Breysse, M., Portefaix, J.-L., & Varinat, M. (1991). *Catal. Today 10*, 489.

[52] P. Michaud, J.L. Lemberton, G. Perot, Hydrodesulfurization of dibenzothiophene and 4,6-dimethyldibenzothiophene: effect of an acid component on the activity of a sulfide NiMo on alumina catalyst, Appl. Catal. A: Gen. 169 (1998) 343–353.

[53] Kresge, C. T., Leonowicz, M. E., Roth, W. J., Vartuli, J. C. and Beck, J. S. (1992) Nature, **359**, 710.

[54] Zhao, D. Y., Feng, J. L., Huo, Q. S., Melosh, N., Fredrickson, G. H., Chmelka, B. F. and Stucky, G. D. (1998) Science, 279, 548.

[55] K. P. de Jonge (editor), Synthesis of solid catalysts, Wiley publication, pp. 277.

[56] Goula, M.A., Kordulis, C., & Lycourghiotis, A. (1992). *J. Catal. 133*, 486.

[57] Sun, M., Nicosia, D., & Rrins, R. (2003). *Catal. Today 86*, 173.

[58] Bezverkhyy, I., Afanasiev, P., & Lacroix, M. (2005). *J. Catal. 230*, 133.

[59] Lee, J. J.; Kim, H.; Moon, S. H. Preparation of highly loaded, dispersed MoS_2/Al_2O_3 catalysts for the deep hydrodesulfurization of dibenzothiophenes. *Appl. Catal., B* 2003, *41*, 171.

[60] Mauge, F., Vallet, A., Bachelier, J., Duchet, J.C., & Lavalley, J.C. (1996). *J. Catal. 162*, 88.

[61] Lee, J.J., Kim, H., Koh, J.H., Jo, A., & Moon, S.H. (2005). *Appl. Catal. B 58*, 89.

[62] K.G. Knudsen, B.H. Cooper, H. Topsoe, Catalyst and process technologies for ultra low sulfur diesel, Appl. Catal. A: Gen. 189 (1999) 205–215.

[63] B.C. Gates, H. Topsoe, Reactivities in deep catalytic hydrodesulfurization: challenges, opportunities, and the importance of 4-methyldibenzothiophene and 4,6-dimethyldibenzothiophene, Polyhedron 16 (1997) 3213–3217.

[64] V. Meille, E. Schulz, M. Lemaire, M. Vrinat, Hydrodesulfurization of alkyldibenzothiophenes over a NiMo/Al2O3 catalyst: kinetics and mechanism, Catal. 170 (1997) 29–36.

[65] H. Farag, D.D. Whitehurst, K. Sakanish, I. Mochida, Catal. Today 50 (1999) 49.

[66] Broderick, B.C. Gates, Hydrogenolysis and hydrogenation of dibenzothiophene catalyzed by sulfided Co–Mo/Al2O3: the reaction kinetics, AIChE J. 27 (1981) 663–673.

[67] Vrinat, M. L., Appl. Catal. 6, 137 (1983).

[68] J. Chen, H. Yang, Z. Ring, HDS kinetics study of dibenzothiophenic compounds in LCO, Catal. Today 98 (2004) 227–233.

[69] I. Bezverkhy, P. Afanasiev, M. Lacroix, Inorg. Chem. 39 (2000) 5416.

[70] P. Afanasiev, G.-F. Xia, G. Berhault, B. Jouguet, M. Lacroix, Chem. Mater. 11 (1999) 3216.

[71] T. Homma, M. Echard, J. Leglise, Catal. Today 106 (2005) 238.

[72] W. H. Zhang, J. Lu, B. Han, M. Li, J. Xiu, P. Ying, C. Li, Chem. Mater. 14 (2002) 3413.

[73] J.A. Melero, J.M. Arsuaga, P. de Frutos, J. Iglesias, J. Sainz, S. Bla´zquez, Micropor. Mesopor. Mater. 86 (2005) 364–373.

[74] S. Wu, Y. Han, Y.-C. Zhou, J.-W. Song, L. Zhao, Y. Di, S.-Z. Liu, F.-S. Xiao, Chem. Mater. 16 (2004) 486–492.

[75] Muthu Kumaran G., Garg S., Soni K., Kumar M., Sharma L. D., Rana Rao K. S., and Murali D. G., Ind. Eng. Chem. Rev. 2007, 46, 4747-4754.G.

[76] Murali Dhar, G. Muthu Kumaran, M. Kumar, K. S. Rawat, L. D. Sharma, B. D. Raju, K. S. Rama Rao, Catalysis Today, 99, (2005), 309-314.

[77] J. Jurapatrakorn, M.P. Coles, T.D. Tilley, Chem. Mater. 17 (2005) 1818–1828.

[78] K. Marcinkowska, L. Rodrigo, S. Kaliaguine and P. C. Roberge, Journal *of* molecular *Catalysis*, 33 (1985) 189 – 200.

[79] Sugino T., Kido A., Azuma N., Ueno A., and Udagawa Y., Journal of Catalysis 190, 118-127 (2000).

[80] Banares M. A., Hu, H., and Waches, I. E., *J. Catal.* **150**, 407 (1994).

[81] Deltcheff, C. R., Amirouche, M., Che, M., Tatibouet, J. T., and Fournier, M., *J. Catal.* **125**, 292 (1990).

[82] Li, C.; Xiu, Q.; Wang, K. L.; Guo, X., FT-IR Emission Spectroscopy Studies of Molybdenum Oxide and Supported Molybdena on Alumina, Silica, Zirconia, and Titania. Appl. Spectrosc. 1991, 45, 874.

[83] F. Sanchez-Minero, J. Ramirez, R. Cuevas-Garcia, A. Gutierrez- Alejandre, C. Fernandez-Vargas, Ind. Eng. Chem. Res. 2009, 48, 1178-1185.

[84] H. Farag, Energy and Fuels, 2006, 20, 1815-1821.

[85] Mochida, I.; Choi, K. *J. Jpn. Petrol. Inst*. **2004**, *47* (3), 145-163.

[86] Daage, M.; Chianelli, R. R. *J. Catal*. **1994**, *194*, 414-427.

VITA

Name	Zakariyah Abdulkareem Jamiu
Mail Address	No. 1, Darus-salaam-Jamiu's Compound, Okaito, Okehi LG, Kogi-Nigeria
Home Address	No. 1, Darus-salaam-Jamiu's Compound, Okaito, Okehi LG, Kogi-Nigeria
Contacts	Mobile: 966556209764 E-mail: gurfatan@gmail.com

Education/Training

June,2004	BS in Applied Chemistry from University of Jos, Nigeria
May,2012	MS in Chemistry from King Fahd University of Petroleum & Minerals, KFUPM, Dhahran-Saudi Arabia

Career History

2009-2012	Worked as research assistant with Chemistry Department, KFUPM
2007-2009	Monitoring & Evaluation Officer with Partners for International Development and Education (PIDE), Nigeria
2005-2006	Worked as a science teacher with Olokoto Community Grammar School, Orire LG, Oyo State-Nigeria
2004-2005	Worked as a science teacher with Hayatul Islam Primary School, Angwa rogo, Jos, Plateau State-Nigeria
2003-2004	Research assistant with National Metallurgical Development Centre, Jos-Nigeria